Title

Heat capacities, entropies, and Gibbs free energies of formation of low-k amorphous Si(O)CH dielectric films and implications for stability during processing

Authors

Chen, Jiewei
Calvin, Jason
Asplund, Megan
et al.

Publication Date

2019

DOI

10.1016/j.jct.2018.08.026

Peer reviewed

J. Chem. Thermodynamics 128 (2019) 320–335

Contents lists available at ScienceDirect

J. Chem. Thermodynamics

journal homepage: www.elsevier.com/locate/jct

Heat capacities, entropies, and Gibbs free energies of formation of low-*k* amorphous Si(O)CH dielectric films and implications for stability during processing

Jiewei Chen [a], Jason Calvin [c], Megan Asplund [c], Sean W. King [b], Brian F. Woodfield [c], Alexandra Navrotsky [a,*]

[a] Peter A. Rock Thermochemistry Laboratory and NEAT ORU, University of California Davis, Davis, CA 95616, United States
[b] Logic Technology Development, Intel Corporation, Hillsboro, OR 97124, United States
[c] Department of Chemistry and Biochemistry, Brigham Young University, Provo, UT 84602, United States

ARTICLE INFO

Article history:
Received 14 March 2018
Received in revised form 15 August 2018
Accepted 16 August 2018
Available online 19 August 2018

Keywords:
Heat capacity
Entropy
Gibbs free energy
Amorphous low-*k* SiOCH films
Formation enthalpy
Thermodynamic stability

ABSTRACT

Low-temperature heat capacities of a series of low dielectric constant amorphous films with different compositions were measured from 1.8 to 300 K using a Quantum Design Physical Property Measurement System (PPMS). By using piece wise functions to fit the heat capacities, the characteristic Debye temperatures Θ_D and the standard molar entropies are determined. The standard molar entropies of these materials range from 8.8 $J{\cdot}K^{-1}{\cdot}mol^{-1}$ to 17.5 $J{\cdot}K^{-1}{\cdot}mol^{-1}$. Together with the formation enthalpies obtained by high temperature oxidative solution calorimetry in molten sodium molybdate solvent, the corresponding Gibbs free energies from elements and crystalline constituents (and gaseous products as required) are obtained. The Gibbs free energy terms of these materials are dominated by the enthalpy term rather than the entropy. These samples are thermodynamically stable at room temperature with respect to elements and the samples with oxygen incorporated are generally thermodynamically more stable than the others. However, compared to crystalline binary counterparts and gases, some of these materials possess either positive or close-to-zero Gibbs free energies of formation, indicating that they are thermodynamically metastable; while, for the rest, which are stable at ambient conditions, elevation of temperature will eventually lead to decomposition.

1. Introduction

There is significant interest in finding new generation low dielectric constant (low-*k*) materials for applications in integrated circuits. New dielectric materials, such as hydrogenated amorphous silicon carbide (a-SiCH) and hydrogenated amorphous silicon oxycarbide (a-SiOCH), show great potential in replacing the traditional SiO_2 as inter-layer dielectrics (ILDs) and etch stop layers (ESLs) [1,2]. In addition to the low dielectric constant [3], these materials show many other desirable properties, such as high temperature stability [4] and enhanced thermal, mechanical, and chemical properties [5–11].

The most commonly used industrial methods to synthesize this new class of low-*k* a-Si(O)CH thin film dielectrics are chemical vapor deposition (CVD) [12] and plasma enhanced CVD (PECVD) [13–15]. To incorporate C and H into the system, various different organosilane or alkoxysilane precursors in combination with strong or weak oxidizers such as O_2, N_2O, and CO_2 are used during the CVD of SiO_2. In general, these methods require lower temperatures (250–600 °C vs. 700–1200 °C), and yields higher hydrogen content than the pyrolysis route (20–45 atomic % vs. less than 10 atomic %), which is another common method [16–19]. More importantly, CVD/PECVD can substantially reduce the dielectric permittivity of a-Si(O)CH films compared to SiO_2 [14,20].

Although these low-*k* dielectrics show chemical stability as deposited, a critical drawback is that they tend to lose hydrogen and carbon (as labile organic groups) and convert to SiO_2 during thermal annealing and other nano-electronic fabrication processes [21–23]. Thus, it is crucial to investigate the thermodynamic stability of these materials and their interfaces with other materials to find processing conditions that do not lead to significant degradation. With increased thermodynamic understanding of these materials, the long-term stability of the products manufactured from them can be improved [24,25]. Our previous work measured the formation enthalpies of related materials [26] by high temperature oxidative solution calorimetry in a molten oxide solvent. The results show that introducing organic functional groups into the

* Corresponding author.
E-mail address: anavrotsky@ucdavis.edu (A. Navrotsky).

https://doi.org/10.1016/j.jct.2018.08.026
0021-9614/

system increases thermodynamic stability by saturating surface bonding and eliminating defects such as dangling bonds. However, there is still a gap in the thermodynamic data since the entropies of formation of these and related materials are not known. Furthermore, low temperature heat capacity measurements can give insight into the vibrational and defect behavior of these complex

Table 1
Film type, compositions, molecular weight, dielectric constant, mass density for different low-k a-Si(O)CH Films. A mole is defined as a gram-atom, that is Avogadro's number of atoms.

Sample #	Film Type	Si[b]	O[b]	C[b]	H[b]	Mass[c] (g·mol^{-1})	Dielectric Constant (k)	Mass Density[d] (g·cm^{-3})
R337[a]	a-SiCH	37.1	0.3	36.3	26.3	15.093	7.2	2.5
300	a-SiCH	21.2	0	32.6	46.3	10.336	5	1.8
844[a]	a-SiOCH	36.1	45.2	10	8.6	18.658	4.2	2.4
539	a-SiOCH	26.7	39.55	12.4	21.34	15.531	3.8	2.2
338	a-SiOCH	20.3	34	15.5	30.2	13.309	3.2	1.6
248[a]	a-SiOCH	25.4	19.6	22.6	32.5	13.312	4.8	2
149	a-SiOCH	16.36	26.1	15.05	42.49	11.007	3.3	1.3
659	a-SiOCH	10.4	10.2	24.1	55.3	8.005	2.6	1.25

[a] Sample 248, R337, 844 are sample #3,4,5 in Ref. [26].
[b] The composition is presented in atomic percentage.
[c] Mass is molar mass.
[d] The uncertainty of mass density is ± 0.1 g/cm^3.

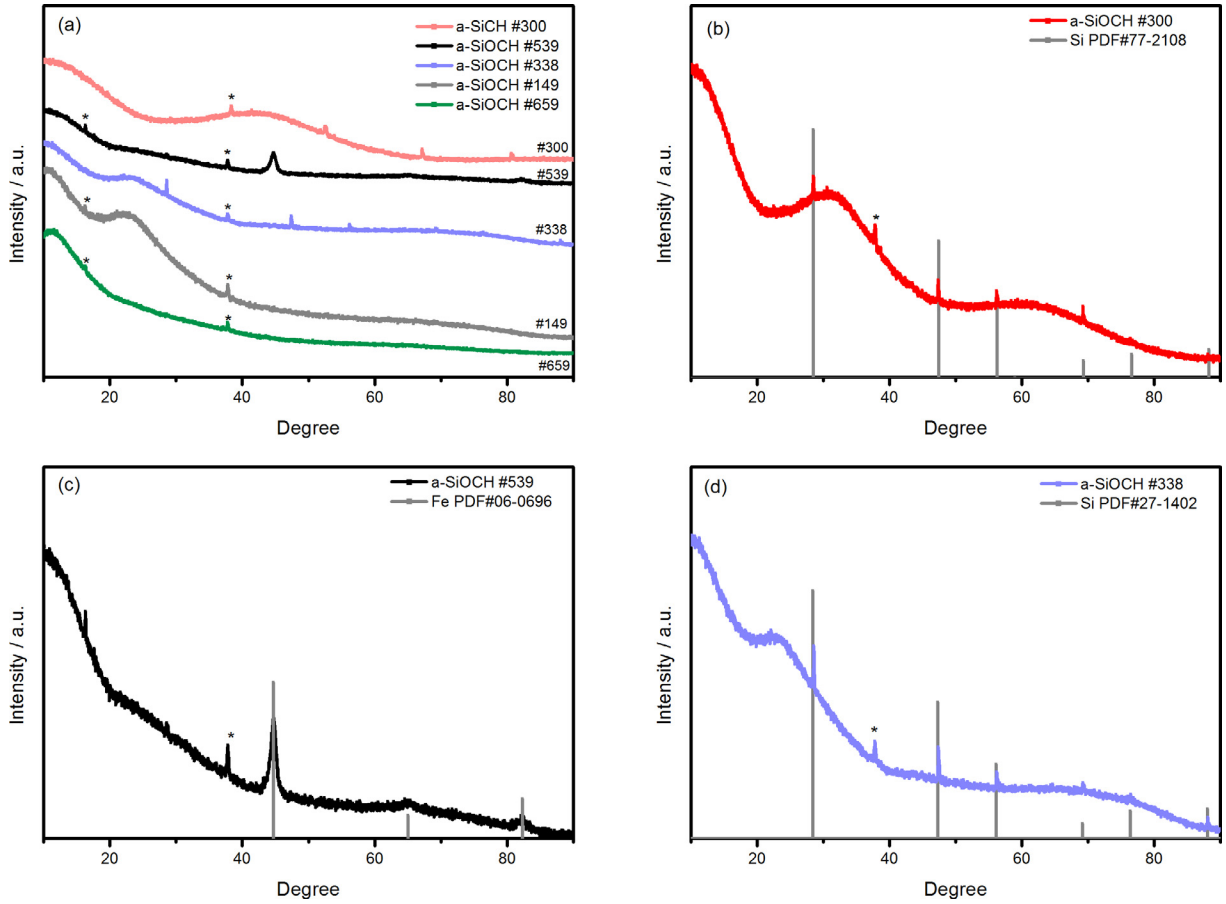

Fig. 1. PXRD patterns of Si(O)CH samples. Peaks arise from sample holder are marked with stars. The crystalline impurities were compared with different reference patterns in (a)–(c).

Table 2
Details of the PPMS calorimetric measurements including pressures (p), sample mass (M_s), molar mass (M), and copper mass (M_{Cu}). The estimated standard uncertainties in the masses $M_{s,Cu}$ and pressure p are $u(M_{s,Cu})$ = 0.06 mg and $u(p)$ = 0.1 mPa.

	#R337	#300	#844	#539	#338	#248	#149	#659
p/mPa	1.2	1.2	1.2	1.2	1.2	1.2	1.2	1.2
M_s/mg	12.98	7.16	9.28	4.02	8.94	11.02	9.84	2.36
M/g·mol^{-1}	15.093	10.336	18.658	15.531	13.309	13.312	11.007	8.005
M_{Cu}/mg	28.76	30.10	25.36	18.20	22.60	32.66	28.96	29.92

Table 3
Pellet mass and Enthalpy of Drop Solution (ΔHds) of each experiment for different samples.

Sample #	300		539		338		149		659	
Experiment number	Pellet mass (mg)	ΔH_{ds} (kJ/mol)	Pellet mass (mg)	ΔH_{ds} (kJ/mol)	Pellet mass (mg)	ΔH_{ds} (kJ/mol)	Pellet mass (mg)	ΔH_{ds} (kJ/mol)	Pellet mass (mg)	ΔH_{ds} (kJ/mol)
1	2.44	−228.34	1.301	−130.18	2.113	−119.38	1.129	−164.65	1.032	−108.97
2	2.49	−232.29	1.111	−129.66	2.680	−118.13	0.873	−162.44	0.941	−108.38
3	1.75	−231.87	1.126	−129.71	2.102	−118.11	1.127	−164.05	0.754	−98.55
4	1.86	−233.95	1.361	−127.43	2.726	−119.42	0.957	−165.26	0.959	−107.88
5	1.92	−230.01	1.168	−126.72	2.471	−119.39	0.658	−163.28	0.839	-115.08
6	1.87	−−228.27	1.057	-125.91	2.783	−117.54	0.842	−163.56	0.696	−110.53
7	2.02	−226.15	0.928	−126.83	1.997	−120.18	0.975	−163.37	0.850	−116.57
8	1.79	−227.21	0.694	−127.84	2.640	−118.22	0.859	−163.26	0.786	−123.60
Average ΔH_{ds} (kJ/mol)	−229.76 ± 1.93(8)		−128.03 ± 1.14(8)		−118.79 ± 0.64(8)		−163.73 ± 0.63(8)		−111.19 ± 5.22(8)	

Table 4
Enthalpies of Drop Solution (ΔH_{ds}), Enthalpies of Oxidation ($\Delta H^0_{ox,\ 25°C}$), Enthalpies of Formation from Elements ($\Delta H^0_{f,\ elem}$), Standard Entropies (S^o), Entropies of Formation from Elements ($\Delta S^0_{f,\ elem}$), Gibbs Free Energies of Formation from Elements ($\Delta G^0_{f,\ elem}$) at Room Temperature for Different Low-k a-Si(O)CH Films. A mole is defined as a gram-atom, that is Avogadro's number of atoms.

Sample #	Film Type	ΔH_{ds} (kJ/mol)	$\Delta H_{ox,25°C}$ (kJ/mol)	$\Delta H_{f,ele}$ (kJ/mol)	S^o (J·K^{-1}·mol^{-1})	$\Delta S^o_{f,ele}$ (J·K^{-1}·mol^{-1})	$\Delta G^o_{f,ele}$ (KJ·mol^{-1})
R337[a]	a-SiCH[b]	−458.32 ± 5.80(7)[c,d]	−479.94 ± 5.80	−37.50 ± 5.85	8.80 ± 0.18	−17.76 ± 0.18	−32.21 ± 5.85
300	a-SiCH	−229.76 ± 1.93(8)	−252.96 ± 1.93	−133.15 ± 1.98	10.59 ± 0.21	−25.50 ± 0.21	−125.55 ± 1.98
844[a]	a-SiOCH	−94.68 ± 0.70(8)	−113.17 ± 0.70	−266.47 ± 1.00	13.02 ± 0.26	−46.34 ± 0.26	−252.66 ± 1.00
539	a-SiOCH	−128.03 ± 1.14(8)	−147.62 ± 1.14	−174.21 ± 1.27	11.18 ± 0.22	−49.07 ± 0.22	−159.58 ± 1.27
338	a-SiOCH	−118.79 ± 0.64(8)	−139.15 ± 0.64	−149.40 ± 0.77	17.46 ± 0.35	−41.86 ± 0.35	−136.92 ± 0.78
248[a]	a-SiOCH	−211.04 ± 2.79(8)	−232.41 ± 2.79	−133.71 ± 2.84	9.66 ± 0.02	−37.75 ± 0.02	−122.45 ± 2.84
149	a-SiOCH	−163.73 ± 0.63(8)	−185.77 ± 0.63	−82.78 ± 0.72	14.40 ± 0.29	−44.08 ± 0.29	−69.64 ± 0.72
659	a-SiOCH	−111.19 ± 5.22(8)	−134.72 ± 5.22	−133.61 ± 5.23	11.77 ± 0.24	−38.17 ± 0.24	−122.23 ± 5.23

[a] Sample 248, R337, 844 are sample #3,4,5 in Ref. [26].
[b] The amount of oxygen is really small and the structural analysis suggests #R337 belongs to a-SiCH film type.
[c] Uncertainty is two standard deviations of the mean.
[d] Number in the parentheses is the number of measurements of each sample.

materials. For industrial applications, accurately obtaining the heat capacity of low-k a-Si(O)CH materials will contribute to determining the thermal conductivity, a parameter which is essential for controlling the heat flow and performance of the devices [27]. Thus, there is a great need to measure and understand the entropy of low-*k* a-Si(O)CH materials to assess their ultimate stability in highly scaled and integrated nano-electronic products. Examination of the complete thermochemistry of low-*k* a-SiOCH materials will also broaden the understanding of the energy landscape in the Si-O-C and Si-O-C-H systems [28–32] by examining previously unexplored portions of these phase diagrams [33–38].

In this context, the goal of this work is to measure low temperature heat capacities ($C_{p,m}$) of these low-*k* Si(O)CH dielectric films and obtain their standard entropies (S^o). Together with the enthalpies of formation obtained previously [26], their Gibbs energies of formation (ΔG^o_f) can be determined, thus providing a complete thermodynamic dataset for these low-*k* Si(O)CH materials. These data are a starting point for further work on other low-*k* amorphous materials with different compositions and structure to provide insight into trends in the stabilities of dielectric films with different compositions and functional groups. The behavior of the heat capacity at low temperature also sheds light on the vibrational density of states and possible dynamic disorder in these materials.

2. Experimental methods

2.1. Sample synthesis and characterization

This is a continuation of previous work, with detailed synthesis and characterization described in [26]. The full elemental compositions and mass density of the SiOCH films were determined by

Table 5
Measured molar heat capacity values at constant pressure[c] for a-SiCH #R337. M = 15.093 g·mol^{-1}.[a]

T/K[b]	$C_{p,m}$/J·K^{-1}·mol^{-1}	T/K[b]	$C_{p,m}$/J·K^{-1}·mol^{-1}	T/K[b]	$C_{p,m}$/J·K^{-1}·mol^{-1}
1.8308	$1.7349\cdot10^{-4}$	8.0373	$2.6511\cdot10^{-3}$	77.385	1.7752
1.9132	$1.9071\cdot10^{-4}$	8.3929	$2.7306\cdot10^{-3}$	84.561	2.1381
1.9982	$1.9211\cdot10^{-4}$	8.7558	$3.8425\cdot10^{-3}$	92.411	2.5332
2.0876	$2.0000\cdot10^{-4}$	9.1379	$4.3333\cdot10^{-3}$	100.97	2.9453
2.1803	$2.2415\cdot10^{-4}$	9.5389	$4.9327\cdot10^{-3}$	111.07	3.4458
2.2788	$2.3379\cdot10^{-4}$	9.9601	$5.1435\cdot10^{-3}$	121.14	3.9665
2.3827	$2.2497\cdot10^{-4}$	10.376	$5.7846\cdot10^{-3}$	131.23	4.4667
2.4878	$2.5047\cdot10^{-4}$	10.779	$6.3448\cdot10^{-3}$	141.31	4.9721
2.6001	$2.3456\cdot10^{-4}$	11.244	$7.0551\cdot10^{-3}$	151.35	5.4986
2.7202	$2.8391\cdot10^{-4}$	11.737	$7.7753\cdot10^{-3}$	161.47	5.9963
2.8599	$2.4371\cdot10^{-4}$	12.256	$9.2256\cdot10^{-3}$	171.51	6.4966
2.9866	$3.0536\cdot10^{-4}$	12.803	0.010979	181.59	7.0244
3.1185	$3.1000\cdot10^{-4}$	13.370	0.012608	191.65	7.5043
3.2531	$3.3062\cdot10^{-4}$	13.954	0.014639	201.78	7.9767
3.4017	$3.7350\cdot10^{-4}$	14.584	0.016899	211.85	8.4347
3.5446	$4.1766\cdot10^{-4}$	15.224	0.019356	221.86	8.8696
3.7035	$4.7246\cdot10^{-4}$	15.717	0.021044	231.92	9.3039
3.8663	$5.0846\cdot10^{-4}$	17.205	0.028280	241.98	9.7016
4.0365	$5.9610\cdot10^{-4}$	18.768	0.037249	252.13	10.140
4.2149	$5.1428\cdot10^{-4}$	20.491	0.047964	262.19	10.533
4.4016	$7.0476\cdot10^{-4}$	22.451	0.059305	272.25	10.910
4.5984	$5.8285\cdot10^{-4}$	24.491	0.081155	282.21	11.323
4.8016	$6.3068\cdot10^{-4}$	26.751	0.10821	292.35	11.674
5.0103	$9.2970\cdot10^{-4}$	29.234	0.13856	302.44	12.098
5.2343	$9.3441\cdot10^{-4}$	31.925	0.18607		
5.4614	$1.0469\cdot10^{-3}$	34.881	0.24419		
5.7042	$1.0111\cdot10^{-3}$	38.103	0.31583		
5.9459	$9.5009\cdot10^{-4}$	41.628	0.40272		
6.2076	$1.2253\cdot10^{-3}$	45.479	0.51890		
6.4859	$1.5260\cdot10^{-3}$	49.692	0.63725		
6.7703	$1.5641\cdot10^{-3}$	54.292	0.79903		

Table 5 (*continued*)

T/K[b]	$C_{p,m}$/J·K^{-1}·mol^{-1}	T/K[b]	$C_{p,m}$/J·K^{-1}·mol^{-1}	T/K[b]	$C_{p,m}$/J·K^{-1}·mol^{-1}
7.0686	$1.8421\cdot10^{-3}$	59.314	0.99136		
7.3747	$1.8876\cdot10^{-3}$	64.811	1.2085		
7.7028	$2.4597\cdot10^{-3}$	70.818	1.4657		

[a] Measurements were performed using a Quantum Design Physical Properties Measurement System (PPMS) with a standard uncertainty of 5% $C_{p,m}$ below T = 20 K and 2% $C_{p,m}$ above T = 20 K.
[b] The uncertainty in temperature is 4 mK.
[c] The pressure was 1.2 mPa during the measurements with uncertainty 0.1 mPa.

combined Rutherford backscattering and nuclear analysis (RBS-NRA) measurements [39]. The elemental composition is listed in percentage with summation of percentage of each element to be 100%. A mole of sample is defined as Avogadro's number of atoms (Si + O + C + H), i.e. a gram atom. Powder X-ray diffraction (PXRD) was done to ensure the amorphous nature of these materials. A summary of sample descriptions is given in Table 1. Note that samples #300, #659, #338, #539, #149 are not from [26], but they were synthesized in a similar fashion.

2.2. Enthalpy of formation measurements

High temperature oxidative molten salt solution calorimetry was utilized to determine the formation enthalpies of the amorphous powders. Similar compounds have been studied previously by the same technique in our laboratory [26] and this methodology is well established [40–42]. In a typical measurement, ~1–2.5 mg pellets were prepared by pressing the powdered samples (obtained after grinding the flakes) into a 1 mm die. The pellets were dropped from room temperature into molten sodium molybdate ($3Na_2O{\cdot}4MoO_3$) solvent maintained at 1073 K inside an AlexSYS Setaram microcalorimeter. To ensure full oxidation and to stir the melt, oxygen gas was constantly bubbled through the solvent with a rate about 5 mL/min. The gaseous products CO_2 and H_2O from oxidation reaction were removed from the system by flushing oxygen gas (~40 mL/min) through the calorimeter assembly. In general, it takes 50–60 min for the calorimetric signal to return back to baseline. The calorimeter was periodically calibrated against the heat content of platinum. Statistically reliable data (within two standard error) were obtained by dropping a number of pellets.

2.3. Heat capacity measurements

The low temperature heat capacities of all eight samples were measured at P = 1.2 mPa using a Quantum Design Physical Property Measurement System (PPMS) with logarithmic spacing from T = 1.8 to 100 K, and 10 K increments from T = (100 to 300) K. Samples were prepared for heat capacity measurement by mixing about 2 to 13 mg of each powder with about 5 mg of copper strips (Alfa Aesar, 0.99999

Table 6
Measured molar heat capacity values at constant pressure[c] for a-SiCH #300. M = 10.336 g·mol^{-1}.[a]

T/K[b]	$C_{p,m}$/J·K^{-1}·mol^{-1}	T/K[b]	$C_{p,m}$/J·K^{-1}·mol^{-1}	T/K[b]	$C_{p,m}$/J·K^{-1}·mol^{-1}
1.8416	$4.7419\cdot10^{-4}$	8.0299	0.032616	77.437	2.8830
1.9154	$5.3450\cdot10^{-4}$	8.3856	0.036509	84.619	3.2602
2.0070	$5.8799\cdot10^{-4}$	8.7509	0.040621	92.471	3.6062
2.1011	$6.5137\cdot10^{-4}$	9.1334	0.045904	101.04	3.9875
2.2018	$7.8927\cdot10^{-4}$	9.5289	0.051450	111.16	4.4404
2.3050	$8.6129\cdot10^{-4}$	9.9459	0.056420	121.22	4.9162
2.4140	$9.5470\cdot10^{-4}$	10.371	0.063676	131.28	5.3205
2.5214	$1.0526\cdot10^{-3}$	10.782	0.070231	141.41	5.7291
2.6199	$1.2288\cdot10^{-3}$	11.249	0.077908	151.46	6.1891
2.7420	$1.4243\cdot10^{-3}$	11.745	0.086338	161.59	6.5941
2.8646	$1.5894\cdot10^{-3}$	12.265	0.096651	171.64	6.9846
2.9894	$1.6106\cdot10^{-3}$	12.808	0.10732	181.73	7.4077
3.1153	$1.9665\cdot10^{-3}$	13.379	0.11913	191.81	7.8154
3.2555	$2.3321\cdot10^{-3}$	13.969	0.13207	201.95	8.2632
3.3998	$2.6236\cdot10^{-3}$	14.581	0.14576	212.03	8.6329
3.5474	$2.8797\cdot10^{-3}$	15.221	0.16089	222.05	9.0099
3.6998	$3.1956\cdot10^{-3}$	15.739	0.17296	232.13	9.3807
3.8600	$4.0013\cdot10^{-3}$	17.178	0.21075	242.19	9.7436
4.0321	$4.4922\cdot10^{-3}$	18.795	0.25464	252.35	10.142
4.2142	$5.1437\cdot10^{-3}$	20.504	0.30442	262.41	10.466
4.3989	$5.7148\cdot10^{-3}$	22.439	0.36493	272.47	10.843
4.5865	$6.4268\cdot10^{-3}$	24.499	0.43246	282.43	11.178
4.7929	$7.0432\cdot10^{-3}$	26.771	0.50931	292.55	11.393
5.0086	$8.4990\cdot10^{-3}$	29.256	0.60110	302.62	11.618
5.2244	$9.4155\cdot10^{-3}$	31.963	0.70628		
5.4571	0.010195	34.909	0.83771		
5.7003	0.012513	38.134	0.97586		
5.9503	0.013978	41.660	1.1360		
6.2134	0.016043	45.519	1.3179		
6.4715	0.017246	49.731	1.5154		
6.7585	0.020222	54.331	1.7222		
7.0620	0.023097	59.357	1.9686		
7.3734	0.025542	64.858	2.2369		
7.6985	0.029666	70.870	2.5415		

[a] Measurements were performed using a Quantum Design Physical Properties Measurement System (PPMS) with a standard uncertainty of 5% $C_{p,m}$ below T = 20 K and 2% $C_{p,m}$ above T = 20 K.
[b] The uncertainty in temperature is 4 mK.
[c] The pressure was 1.2 mPa during the measurements with uncertainty 0.1 mPa.

Table 7
Measured molar heat capacity values at constant pressure[c] for a-SiOCH #844. M = 18.658 g·mol^{-1}.[a]

T/K[b]	$C_{p,m}$/J·K^{-1}·mol^{-1}	T/K[b]	$C_{p,m}$/J·K^{-1}·mol^{-1}	T/K[b]	$C_{p,m}$/J·K^{-1}·mol^{-1}
1.8276	$1.7110\cdot10^{-4}$	8.0332	0.012922	77.365	3.4186
1.9155	$2.0113\cdot10^{-4}$	8.3872	0.014958	84.541	3.9063
2.0031	$2.1548\cdot10^{-4}$	8.7527	0.016326	92.386	4.4117
2.1007	$2.3176\cdot10^{-4}$	9.1374	0.021308	100.95	4.9142
2.2002	$2.6004\cdot10^{-4}$	9.5345	0.024440	111.05	5.5117
2.3043	$2.7815\cdot10^{-4}$	9.9530	0.027240	121.13	6.1386
2.4019	$3.1439\cdot10^{-4}$	10.373	0.032775	131.18	6.6760
2.5040	$3.2651\cdot10^{-4}$	10.776	0.037505	141.30	7.2462
2.6161	$3.5737\cdot10^{-4}$	11.241	0.043062	151.34	7.8078
2.7314	$3.8040\cdot10^{-4}$	11.733	0.049615	161.47	8.3198
2.8534	$4.9900\cdot10^{-4}$	12.252	0.058126	171.51	8.8496
2.9786	$4.9855\cdot10^{-4}$	12.799	0.068037	181.59	9.3837
3.1081	$5.7585\cdot10^{-4}$	13.363	0.078516	191.65	9.9026
3.2468	$5.6040\cdot10^{-4}$	13.953	0.090633	201.79	10.372
3.3927	$7.7609\cdot10^{-4}$	14.568	0.10389	211.86	10.830
3.5431	$7.6496\cdot10^{-4}$	15.209	0.11918	221.88	11.300
3.7011	$9.6929\cdot10^{-4}$	15.721	0.13138	231.95	11.726
3.8622	$1.0971\cdot10^{-3}$	17.170	0.17112	242.01	12.107
4.0319	$1.1434\cdot10^{-3}$	18.780	0.21976	252.17	12.530
4.2145	$1.2777\cdot10^{-3}$	20.486	0.27725	262.23	12.929
4.4004	$1.5082\cdot10^{-3}$	22.446	0.34133	272.29	13.303
4.5939	$1.6807\cdot10^{-3}$	24.484	0.42678	282.26	13.774
4.7952	$1.8407\cdot10^{-3}$	26.741	0.52792	292.39	14.122
5.0114	$2.5072\cdot10^{-3}$	29.222	0.63755	302.48	14.602
5.2314	$2.8835\cdot10^{-3}$	31.911	0.77492		
5.4611	$3.4152\cdot10^{-3}$	34.866	0.92795		
5.6970	$3.5860\cdot10^{-3}$	38.089	1.0994		
5.9424	$4.5304\cdot10^{-3}$	41.613	1.2935		
6.2082	$5.0088\cdot10^{-3}$	45.466	1.5214		
6.4816	$6.1706\cdot10^{-3}$	49.681	1.7378		
6.7671	$6.6057\cdot10^{-3}$	54.279	2.0146		
7.0639	$7.7344\cdot10^{-3}$	59.298	2.3122		
7.3758	$9.4189\cdot10^{-3}$	64.795	2.6370		
7.7002	0.010256	70.797	3.0019		

[a] Measurements were performed using a Quantum Design Physical Properties Measurement System (PPMS) with a standard uncertainty of 5% $C_{p,m}$ below T = 20 K and 2% $C_{p,m}$ above T = 20 K.
[b] The uncertainty in temperature is 4 mK.
[c] The pressure was 1.2 mPa during the measurements with uncertainty 0.1 mPa.

mass fraction purity) to provide better thermal contact and putting this into copper cups (about 15 mg). The cups were then pressed into pellets approximately 3 mm in diameter and 1 mm in height. After running an addenda measurement, which accounts for the heat capacities of the calorimeter and the Apeizon N grease used to mount the sample, a sample was mounted onto the PPMS puck, and the heat capacity was measured. The PPMS automatically corrects for the addenda heat capacity, and the copper contribution was subtracted using data from Ref. [43] yielding the constant pressure heat capacities of SiOCH amorphous materials. The uncertainties for the PPMS measurements of the standard molar heat capacities $C^{o}_{p,m}$, following this method are estimated to be ± 0.02 $C^{o}_{p,m}$ for 1.8 K < T < 10 K and ± 0.01 $C^{o}_{p,m}$ for 10 K < T < 302 K [44]. The molar mass of each sample is given in Table 1.

3. Results and discussion

3.1. XRD characterization

The PXRD patterns of all samples, except for those from Ref. [26] are presented in Fig. 1. Sample #149 and #659 are completely X-ray amorphous without any additional peaks, excluding the peaks from the holder. The rest of the samples (#300, #539, #338) showed the existence of small amounts of crystalline impurities. The crystalline impurities are found to be Si, which serves as the substrate for deposition, or Fe, which comes from the razor blade used for scrapping the sample. The influence of Cu impurities was discussed in [26] and similar argument holds for the Fe impurity, which will not significantly change the result. In the following discussion, we decided to treat these samples with crystalline impurities as a whole, meaning that the thermodynamic parameters of these samples are determined using the overall composition of the amorphous and crystalline mixture, for the following reasons. First, the elemental composition of crystalline impurity Si is the same as those of samples, so it is hard to quantitatively determine their percentage. Second, the heat effects associated with these crystalline impurities are comparable to those of the samples, thus the corresponding results computed from the overall composition will not be significantly different. Lastly, in practical usage of these low-k films, these mixtures are commonly seen and it is reasonable to analysis their stability as a whole.

3.2. Enthalpies of formation

The experimental details, including pellet masses and enthalpies of drop solution calculated from experiments are presented in Table 3. The detailed calculation of enthalpy of formation using appropriate thermodynamic cycles is described in previous work [26]. The enthalpies of drop solution at 800 °C, the enthalpies of oxidation at room temperature, and the enthalpies of formation at room temperature from elements of the newly measured samples are listed in Table 4.

Table 8
Measured molar heat capacity values at constant pressure[c] for a-SiOCH #539. M = 15.531 g·mol^{-1}.[a]

T/K[b]	$C_{p,m}$/J·K^{-1}·mol^{-1}	T/K[b]	$C_{p,m}$/J·K^{-1}·mol^{-1}	T/K[b]	$C_{p,m}$/J·K^{-1}·mol^{-1}
1.8686	5.0650·10^{-4}	7.6746	0.011006	77.213	2.9862
1.9081	5.2908·10^{-4}	8.0228	0.012848	84.356	3.4424
1.9681	5.6280·10^{-4}	8.3849	0.015081	92.222	3.8405
2.0442	6.0505·10^{-4}	8.7632	0.017625	100.79	4.2153
2.1263	6.4999·10^{-4}	9.1595	0.020608	110.91	4.7653
2.2137	7.0212·10^{-4}	9.5732	0.024060	120.94	5.2999
2.3050	7.4837·10^{-4}	10.024	0.028495	131.06	5.7648
2.3994	7.8883·10^{-4}	10.553	0.033670	141.13	6.2487
2.4975	8.3250·10^{-4}	11.065	0.039336	151.19	6.7210
2.5994	8.6856·10^{-4}	11.573	0.045589	161.32	7.1613
2.7079	8.9490·10^{-4}	12.093	0.052411	171.43	7.6002
2.8195	9.1873·10^{-4}	12.632	0.060241	181.49	8.0480
2.9343	9.4137·10^{-4}	13.192	0.069121	191.57	8.4743
3.0243	9.6978·10^{-4}	13.772	0.079607	201.68	8.8606
3.1359	1.0145·10^{-3}	14.390	0.090735	211.78	9.2359
3.2799	1.0933·10^{-3}	15.015	0.10368	221.86	9.5879
3.4657	1.2358·10^{-3}	15.524	0.11431	231.95	9.8882
3.6181	1.3353·10^{-3}	16.977	0.14800	242.03	10.230
3.7774	1.4959·10^{-3}	18.569	0.18881	252.12	10.614
3.9469	1.5876·10^{-3}	20.220	0.23464	262.22	10.892
4.1246	1.7525·10^{-3}	22.200	0.29639	272.33	11.313
4.3086	1.9458·10^{-3}	24.257	0.36569	282.42	11.632
4.4996	2.1625·10^{-3}	26.523	0.45062	292.51	11.864
4.7121	2.3713·10^{-3}	28.936	0.54092	302.62	12.523
4.9240	2.7043·10^{-3}	31.666	0.65065		
5.1497	2.9705·10^{-3}	34.648	0.78810		
5.3832	3.4577·10^{-3}	37.876	0.93619		
5.6256	3.8579·10^{-3}	41.387	1.0969		
5.8784	4.5842·10^{-3}	45.263	1.3084		
6.1434	5.1700·10^{-3}	49.485	1.5048		
6.4496	6.0299·10^{-3}	54.088	1.7285		
6.7334	7.1846·10^{-3}	59.127	1.9856		
7.0315	8.0723·10^{-3}	64.634	2.2780		
7.3449	9.4145·10^{-3}	70.636	2.6017		

[a] Measurements were performed using a Quantum Design Physical Properties Measurement System (PPMS) with a standard uncertainty of 5% $C_{p,m}$ below T = 20 K and 2% $C_{p,m}$ above T = 20 K.
[b] The uncertainty in temperature is 4 mK.
[c] The pressure was 1.2 mPa during the measurements with uncertainty 0.1 mPa.

Table 9
Measured molar heat capacity values at constant pressure[c] for a-SiOCH #338. M = 13.309 g·mol^{-1}.[a]

T/K[b]	$C_{p,m}$/J·K^{-1}·mol^{-1}	T/K[b]	$C_{p,m}$/J·K^{-1}·mol^{-1}	T/K[b]	$C_{p,m}$/J·K^{-1}·mol^{-1}
1.8169	1.1247·10^{-3}	7.6516	0.085943	77.185	5.4990
1.8728	1.2306·10^{-3}	7.9981	0.096137	84.324	6.1014
1.9248	1.3423·10^{-3}	8.3609	0.10722	92.172	6.6734
1.9905	1.4873·10^{-3}	8.7411	0.11938	100.76	7.2186
2.0548	1.6482·10^{-3}	9.1377	0.13269	110.89	7.8894
2.1250	1.8389·10^{-3}	9.5519	0.14724	120.92	8.5145
2.1994	2.0736·10^{-3}	10.122	0.16865	131.01	9.0615
2.2776	2.3070·10^{-3}	10.602	0.18659	141.10	9.5886
2.4311	2.8562·10^{-3}	11.075	0.20508	151.17	10.093
2.5311	3.2333·10^{-3}	11.554	0.22508	161.32	10.549
2.6391	3.6969·10^{-3}	12.076	0.24634	171.38	11.010
2.7515	4.1781·10^{-3}	12.610	0.26969	181.45	11.453
2.8715	4.7613·10^{-3}	13.172	0.29511	191.52	11.891
3.0012	5.4740·10^{-3}	13.757	0.32260	201.61	12.271
3.1356	6.2763·10^{-3}	14.365	0.35242	211.69	12.641
3.2788	7.2169·10^{-3}	15.006	0.38418	221.77	13.005
3.4267	8.3573·10^{-3}	15.510	0.40986	231.84	13.341
3.5955	9.7512·10^{-3}	16.960	0.48663	241.92	13.689
3.7659	0.011288	18.540	0.57459	251.99	14.019
3.9355	0.012995	20.229	0.67109	262.07	14.312
4.1122	0.014928	22.174	0.79327	272.17	14.655
4.2962	0.017101	24.239	0.92961	282.26	14.917
4.5003	0.019683	26.455	1.0898	292.32	15.229
4.6988	0.022362	28.938	1.2683	302.42	15.539
4.9098	0.025405	31.651	1.4780		
5.1291	0.028866	34.610	1.7261		
5.3617	0.032829	37.844	2.0035		
5.6033	0.037235	41.380	2.3106		
5.8566	0.042240	45.242	2.6763		
6.1212	0.047741	49.453	3.0578		
6.4261	0.054417	54.057	3.4707		
6.7084	0.061137	59.100	3.9230		
7.0050	0.068436	64.608	4.4121		
7.3198	0.076844	70.613	4.9330		

[a] Measurements were performed using a Quantum Design Physical Properties Measurement System (PPMS) with a standard uncertainty of 5% $C_{p,m}$ below T = 20 K and 2% $C_{p,m}$ above T = 20 K.
[b] The uncertainty in temperature is 4 mK.
[c] The pressure was 1.2 mPa during the measurements with uncertainty 0.1 mPa.

All samples show negative formation enthalpies from elements at room temperature, ranging from −37 kJ/mol to −266 kJ/mol. In general, samples with oxygen show more negative enthalpies of formation from elements at room temperature, than those without oxygen, which is in consistent with our previous conclusion that oxygen is one of the factors that stabilizes the system thermodynamically.

3.3. Heat capacity curve fitting

The details of the PPMS calorimetric measurements including pressures (p), sample mass (M_s), molar mass (M), and copper mass (M_{Cu}) are presented in Table 2. The measured heat capacities of a-Si(O)CH materials are shown in Tables 5–12 and Figs. 2 and 3. The smoothness in all these curves indicates that no phase transitions happened in this temperature range. All samples show the similar pattern. Fig. 2b emphasizes the behavior of these samples at low temperatures (0–10 K).

Heat capacities were fit to a series of overlapping functions in the low (T < 15 K), mid (5 K < T < 60 K), and high (T > 50 K) temperature regions. The low temperature heat capacity values were fit to the function:

$$C = \gamma T + B_3T^3 + B_5T^5 + B_7T^7 + B_9T^9 + B_{gap}Te^{-\frac{\delta}{2T}}$$

where γ is proportional to the concentration of lattice vacancies in insulating materials [45], and the B_3, B_5, B_7 and B_9 terms represent the harmonic-lattice expression [46]. The final term in the equation accounts for a gap in the Debye density of states model, and was required to fit some of the materials. This model was developed to fit materials with excess low energy vibrational modes. For these materials, a one-dimensional gapped model was used. More information of these gapped models can be found in [47]. The fitting parameters, % RMS, and ranges of validity for these fits as well as those of the mid and high temperature regions are given in Table 13.

The functions used for fitting the mid temperature values were polynomials that have no physical meaning but merely serve to link the low and high temperature fits:

$$C = \sum_{n=0,1,2\cdots7} A_nT^n$$

The high temperature fits consist of a sum of Debye and Einstein heat capacity functions of the form [48]:

$$C = n\hat{A}\cdot D\left(\frac{\Theta_D}{T}\right) + m\hat{A}\cdot E\left(\frac{\Theta_E}{T}\right) + A_1T + A_2T^2$$

where $D(\Theta_D/T)$ and$E(\Theta_E/T))$ are Debye and Einstein functions; m, n,Θ_D , Θ_E, A_1, and A_2 are all adjustable parameters; $m + n$ should be approximately equal to the number of atoms in the formula unit or unit cell. The linear and quadratic terms account for the conversion from constant volume heat capacity to constant pressure heat capacity. The terms obtained from the fitting are summarized in Table 13.

Table 10
Measured molar heat capacity values at constant pressure[c] for a-SiOCH #248. M = 13.312 g·mol^{-1}.[a]

T/K[b]	$C_{p,m}$/J·K^{-1}·mol^{-1}	T/K[b]	$C_{p,m}$/J·K^{-1}·mol^{-1}	T/K[b]	$C_{p,m}$/J·K^{-1}·mol^{-1}
1.8329	$1.5039\cdot10^{-4}$	8.0298	$7.3698\cdot10^{-3}$	77.378	2.4399
1.9134	$1.8233\cdot10^{-4}$	8.3797	$8.8359\cdot10^{-3}$	84.559	2.8088
1.9976	$1.8886\cdot10^{-4}$	8.7436	0.010184	92.406	3.2001
2.0865	$1.9484\cdot10^{-4}$	9.1310	0.012592	100.97	3.5811
2.1794	$2.3238\cdot10^{-4}$	9.5322	0.013615	111.07	4.0420
2.3016	$2.5154\cdot10^{-4}$	9.9457	0.016642	121.06	4.5127
2.4037	$2.8485\cdot10^{-4}$	10.367	0.018824	131.23	4.9514
2.5007	$2.8668\cdot10^{-4}$	10.773	0.021431	141.27	5.3726
2.6266	$2.6794\cdot10^{-4}$	11.240	0.024478	151.39	5.8402
2.7306	$3.3291\cdot10^{-4}$	11.734	0.027973	161.47	6.2465
2.8566	$3.4918\cdot10^{-4}$	12.254	0.032530	171.51	6.6729
2.9802	$4.1734\cdot10^{-4}$	12.797	0.037891	181.63	7.1090
3.1127	$5.0510\cdot10^{-4}$	13.366	0.043686	191.69	7.5234
3.2461	$5.2876\cdot10^{-4}$	13.953	0.050276	201.77	7.9155
3.3931	$5.5606\cdot10^{-4}$	14.568	0.057871	211.84	8.3097
3.5416	$5.8019\cdot10^{-4}$	15.219	0.066318	221.91	8.6846
3.6947	$7.6103\cdot10^{-4}$	15.725	0.072699	231.97	9.0453
3.8580	$6.9904\cdot10^{-4}$	17.170	0.094841	242.03	9.3908
4.0295	$9.1448\cdot10^{-4}$	18.780	0.12234	252.03	9.7470
4.2079	$9.9649\cdot10^{-4}$	20.489	0.15599	262.09	10.090
4.3956	$1.0464\cdot10^{-3}$	22.427	0.19805	272.21	10.413
4.5858	$1.4825\cdot10^{-3}$	24.490	0.24365	282.26	10.793
4.7900	$1.5643\cdot10^{-3}$	26.748	0.31178	292.22	11.110
5.0021	$1.5103\cdot10^{-3}$	29.235	0.37526	302.38	11.441
5.2237	$1.7840\cdot10^{-3}$	31.919	0.46690		
5.4517	$2.5770\cdot10^{-3}$	34.874	0.57195		
5.6944	$2.7079\cdot10^{-3}$	38.097	0.69158		
5.9414	$3.0364\cdot10^{-3}$	41.622	0.82903		
6.1966	$3.0600\cdot10^{-3}$	45.476	0.99326		
6.4752	$3.6777\cdot10^{-3}$	49.689	1.1545		
6.7588	$4.6440\cdot10^{-3}$	54.290	1.3622		
7.0556	$5.6665\cdot10^{-3}$	59.308	1.5859		
7.3650	$5.6073\cdot10^{-3}$	64.807	1.8376		
7.6877	$7.2841\cdot10^{-3}$	70.811	2.1195		

[a] Measurements were performed using a Quantum Design Physical Properties Measurement System (PPMS) with a standard uncertainty of 5% $C_{p,m}$ below T = 20 K and 2% $C_{p,m}$ above T = 20 K.
[b] The uncertainty in temperature is 4 mK.
[c] The pressure was 1.2 mPa during the measurements with uncertainty 0.1 mPa.

Table 11
Measured molar heat capacity values at constant pressure[c] for a-SiOCH #149. M = 11.007 g·mol^{-1}.[a]

T/K[b]	$C_{p,m}$/J·K^{-1}·mol^{-1}	T/K[b]	$C_{p,m}$/J·K^{-1}·mol^{-1}	T/K[b]	$C_{p,m}$/J·K^{-1}·mol^{-1}
1.8307	$2.4771\cdot10^{-3}$	7.8230	0.15247	77.289	4.3754
1.9043	$2.7607\cdot10^{-3}$	8.1625	0.16839	84.441	4.8194
1.9783	$3.2028\cdot10^{-3}$	8.5243	0.18438	92.311	5.2604
2.0596	$3.6728\cdot10^{-3}$	8.9025	0.20185	100.88	5.6646
2.1452	$4.1688\cdot10^{-3}$	9.2982	0.22032	110.96	6.1575
2.2321	$4.8327\cdot10^{-3}$	9.7111	0.24066	121.03	6.6554
2.3269	$5.5812\cdot10^{-3}$	10.214	0.26679	131.16	7.0866
2.4214	$6.4132\cdot10^{-3}$	10.680	0.29032	141.24	7.5030
2.5224	$7.3609\cdot10^{-3}$	11.151	0.31504	151.30	7.9184
2.6281	$8.5760\cdot10^{-3}$	11.644	0.34096	161.43	8.2836
2.7385	$9.3981\cdot10^{-3}$	12.158	0.36869	171.56	8.6661
2.8571	0.010747	12.694	0.39811	181.64	9.0545
2.9939	0.012292	13.255	0.42969	191.73	9.4051
3.1346	0.014090	13.841	0.46424	201.83	9.7414
3.2748	0.016101	14.453	0.50035	211.92	10.052
3.4190	0.018446	15.092	0.53791	222.01	10.353
3.5707	0.020881	15.594	0.56635	232.10	10.645
3.7279	0.023807	17.043	0.65289	242.18	10.951
3.8933	0.026909	18.629	0.74900	252.28	11.248
4.0676	0.030543	20.327	0.86145	262.39	11.511
4.2497	0.034626	22.265	0.96951	272.49	11.727
4.4458	0.039072	24.333	1.0965	282.61	12.022
4.6389	0.043630	26.570	1.2374	292.73	12.294
4.8490	0.048930	29.045	1.3856	302.88	12.577
5.0629	0.054877	31.751	1.5517		
5.2882	0.061012	34.710	1.7422		
5.5281	0.068252	37.944	1.9490		
5.7665	0.076027	41.476	2.1719		
6.0227	0.084405	45.337	2.4210		
6.2906	0.093899	49.558	2.6774		
6.5700	0.10365	54.164	2.9718		
6.8617	0.11438	59.198	3.3020		
7.1643	0.12625	64.692	3.6245		
7.4836	0.14505	70.710	3.9750		

[a] Measurements were performed using a Quantum Design Physical Properties Measurement System (PPMS) with a standard uncertainty of 5% $C_{p,m}$ below T = 20 K and 2% $C_{p,m}$ above T = 20 K.
[b] The uncertainty in temperature is 4 mK.
[c] The pressure was 1.2 mPa during the measurements with uncertainty 0.1 mPa.

Table 12
Measured molar heat capacity values at constant pressure[c] for a-SiOCH #659. M = 8.005 g·mol^{-1}.[a]

T/K[b]	$C_{p,m}$/J·K^{-1}·mol^{-1}	T/K[b]	$C_{p,m}$/J·K^{-1}·mol^{-1}	T/K[b]	$C_{p,m}$/J·K^{-1}·mol^{-1}
1.8304	2.2792·10^{-3}	7.9815	0.12460	77.414	3.5423
1.9109	2.5954·10^{-3}	8.3309	0.13583	84.597	3.9197
1.9978	3.0047·10^{-3}	8.6979	0.15119	92.442	4.2906
2.0879	3.6034·10^{-3}	9.0794	0.16363	101.02	4.5678
2.1834	4.1910·10^{-3}	9.4765	0.17260	111.15	5.0421
2.2807	4.3040·10^{-3}	9.8935	0.19352	121.22	5.4532
2.3835	5.2567·10^{-3}	10.327	0.20747	131.28	5.7921
2.4887	5.9560·10^{-3}	10.756	0.22393	141.41	6.1180
2.5958	7.0307·10^{-3}	11.228	0.24123	151.47	6.4796
2.7185	7.9172·10^{-3}	11.724	0.26025	161.60	6.7827
2.8322	8.9634·10^{-3}	12.243	0.28104	171.65	7.2509
2.9601	0.010916	12.783	0.30353	181.74	7.4788
3.0884	0.011247	13.351	0.32721	191.84	7.7793
3.2249	0.013075	13.938	0.35277	202.01	8.0751
3.3674	0.015183	14.552	0.37869	211.66	8.3402
3.5149	0.016987	15.193	0.40693	222.12	8.6574
3.6672	0.018947	15.703	0.42820	232.19	8.9508
3.8304	0.021928	17.150	0.49278	242.26	9.2176
3.9996	0.024659	18.749	0.56360	252.43	9.6157
4.1749	0.027657	20.475	0.63957	262.50	9.8062
4.3626	0.031567	22.389	0.73574	272.59	10.023
4.5541	0.033991	24.454	0.82532	282.60	10.428
4.7534	0.038873	26.723	0.94031	292.77	10.690
4.9654	0.044027	29.207	1.0309	302.89	10.960
5.1840	0.048493	31.907	1.1687		
5.4157	0.054034	34.861	1.3282		
5.6523	0.060352	38.088	1.4954		
5.9035	0.063842	41.619	1.6816		
6.1554	0.073242	45.478	1.8904		
6.4292	0.077766	49.691	2.1002		
6.7145	0.088555	54.297	2.3248		
7.0101	0.093210	59.337	2.6111		
7.3193	0.10688	64.838	2.9177		
7.6420	0.11785	70.848	3.2170		

[a] Measurements were performed using a Quantum Design Physical Properties Measurement System (PPMS) with a standard uncertainty of 5% $C_{p,m}$ below T = 20 K and 2% $C_{p,m}$ above T = 20 K.
[b] The uncertainty in temperature is 4 mK.
[c] The pressure was 1.2 mPa during the measurements with uncertainty 0.1 mPa.

3.4. Thermodynamic calculations and phase stability

Once fits to all data were completed, smoothed heat capacities and thermodynamic values were generated and are given in Tables 14–21. These thermodynamic values calculated from the fit heat capacity method have an uncertainty of approximately ± 5% below 20 K and ± 2% above 20 K. The standard molar entropies of all samples are quite similar (see Table 4). Fig. 4 suggests a weak linear trend between standard molar entropies at 298 K and O/Si ratio. Note that the two points on the left are two samples without oxygen or with trace amount of oxygen. In general, the standard molar entropies at 298 K increase as O/Si ratio increases. However, no obvious trend was found when plotting the standard molar entropies against other compositional parameters. The influence of composition on entropy is complicated and needs further analysis.

The heat capacities, combined with spectroscopic studies, also can give information on the nature of the lattice vibrations and the vibrational density of states. Such microscopic level interpretation will be pursued in a future study.

By subtracting the entropies of the films from the appropriately weighted average of entropies of the constituent elements, the formation entropies from elements can be computed. Then the corresponding Gibbs free energies can be calculated by using the measured enthalpies and entropies of formation from elements at room temperature. The $\Delta H_{f,ele}$ and $\Delta G_{f,ele}$ values shows that, in general, a-SiOCH are thermodynamically more stable than a-SiCH, which is consistent with our previous findings. The fact that Gibbs free energies follow the same trend as enthalpies of formation validates the argument in our previous study that the enthalpic term, compared to the entropic term, dominates the Gibbs free energy.

Using these data, the formation enthalpies, entropies and Gibbs free energies from solid (cristobalite, SiC, C)/and gaseous compounds (H_2) are calculated, defined by reaction (1).

$$\left(a-\frac{b}{2}\right)\mathrm{SiC(solid,25\,^{\circ}C)}+\frac{b}{2}\mathrm{SiO2(cristobalite,25\,^{\circ}C)}+\left(c-a+\frac{b}{2}\right)\mathrm{C(solid,25\,^{\circ}C)}+\frac{d}{2}\mathrm{H2(gas,25\,^{\circ}C)}\rightarrow \mathrm{SiaObCcHd(solid,25\,^{\circ}C)} \quad (1)$$

The thermocycles for calculation is presented in [26] and the results are summarized in Table 22. Compared to the binary compounds, some of these amorphous films are not energetically stable. Even for those possessing a negative enthalpy term, due to the negative entropy value, reaction (1) will become unfavorable in free energy with increasing temperature. The minimum temperatures for decomposition at 1 atm hydrogen pressure are listed as T_{decomp} in Table 22. Except for sample #300 and #659, all the other samples are thermodynamically favored to decompose either at or below ambient conditions or by the processing temperature

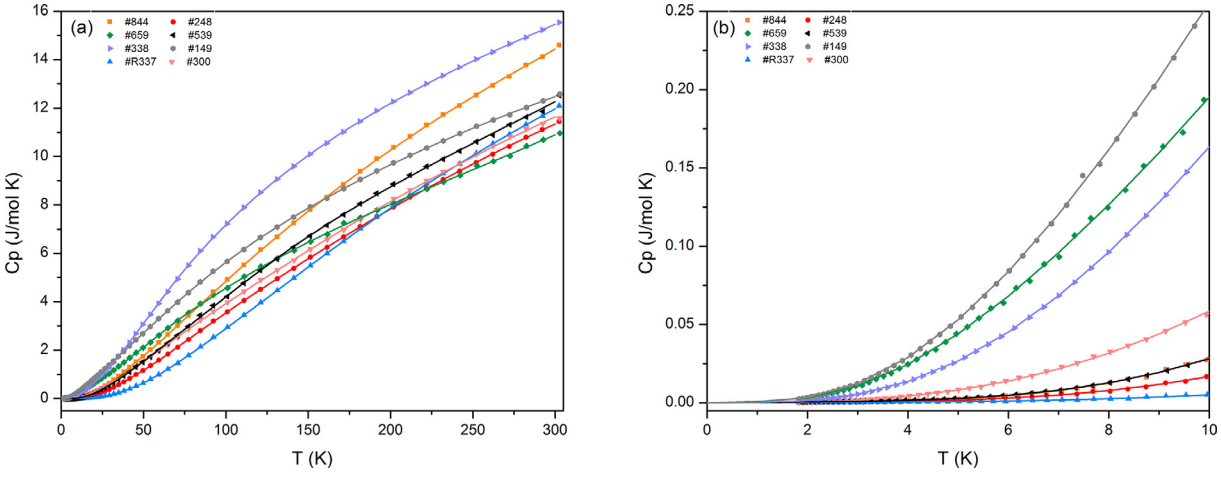

Fig. 2. Experimental heat capacity (dots in each figure) and fitted curves from (a) 0 to 300 K and (b) 0 to 10 K.

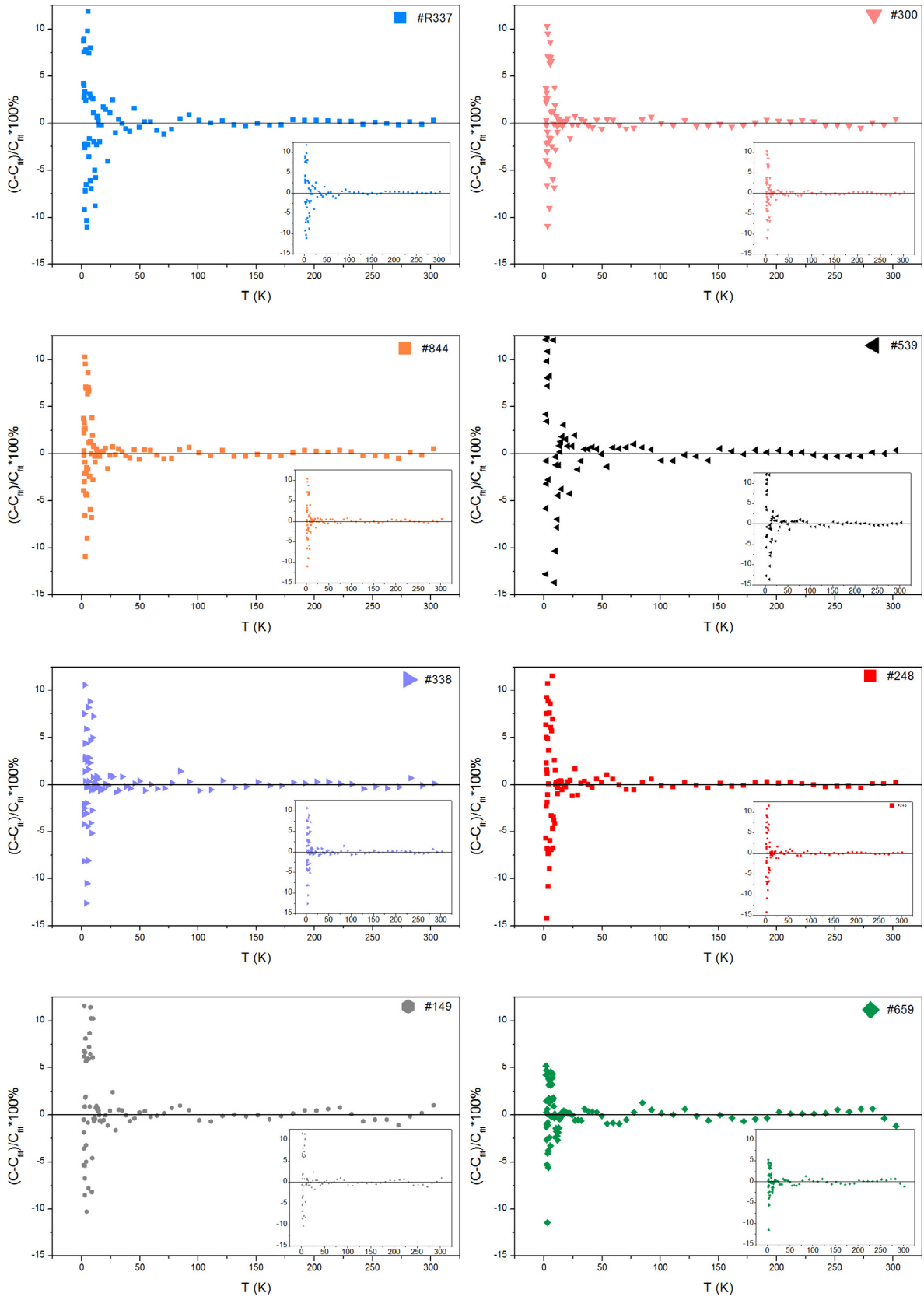

Fig. 3. Percent deviation for different samples.

(400–900 K). In reality, the decomposition will probably be gradual, and the hydrogen pressure generated during decomposition will depend on experimental conditions. It should be noted that since the films are amorphous, one expects an additional positive contribution to their entropy from configurational disorder. Although there is no direct way of assessing this configurational

Table 13
Parameters for low T (<15°K), mid T (10°K < T < 60°K), and high T (T > 50°K) fits of heat capacity data ($J{\cdot}K^{-1}{\cdot}mol^{-1}$) for all SiOCH samples.

	Parameter	#R337	#300	#844	#539	#338	#248	#149	#659
Low T Fits	$\gamma/J{\cdot}K^{-2}{\cdot}mol^{-1}$	$8.32{\cdot}10^{-5}$	$2.43{\cdot}10^{-5}$	$6.27{\cdot}10^{-5}$	0.000281	0	$6.01{\cdot}10^{-5}$	0	0.000829
	$B_3/J{\cdot}K^{-4}$	$2.20{\cdot}10^{-6}$	$6.13{\cdot}10^{-5}$	$9.41{\cdot}10^{-6}$	$2.07{\cdot}10^{-6}$	0.000187	$7.52{\cdot}10^{-6}$	0.000342	$1.80{\cdot}10^{-5}$
	$B_5/J{\cdot}K^{-6}$	$2.72{\cdot}10^{-8}$	$-5.60{\cdot}10^{-8}$	$3.01{\cdot}10^{-7}$	$4.15{\cdot}10^{-7}$	$-9.70{\cdot}10^{-7}$	$1.53{\cdot}10^{-7}$	$-2.30{\cdot}10^{-6}$	$-1.20{\cdot}10^{-8}$
	$B_7/J{\cdot}K^{-8}$	$-6.80{\cdot}10^{-11}$	$-1.90{\cdot}10^{-10}$	$-1.40{\cdot}10^{-9}$	$-2.20{\cdot}10^{-9}$	$2.92{\cdot}10^{-9}$	$-8.50{\cdot}10^{-10}$	$7.43{\cdot}10^{-09}$	0
	$B_9/J{\cdot}K^{-10}$	0	0	$2.46{\cdot}10^{-12}$	$4.22{\cdot}10^{-12}$	0	$1.72{\cdot}10^{-12}$	0	0
	$B_{gap}/J{\cdot}K^{-2}$	0	0	0	0	0.01610	0	0.01498	0.03828
	δ/K	0	0	0	0	12.8134	0	7.4378	8.1167
	%RMS	8.6255	3.2713	4.6204	3.0053	0.5824	6.7304	1.3592	2.4267
	Range/K	1.83–12.87	1.84–13.55	1.83–11.77	1.86–12.41	1.82–6.35	1.83–11.87	1.83–7.93	1.83–11.09
Mid T Fits	$A_0/J{\cdot}K^{-1}{\cdot}mol^{-1}$	0.1663	0.02501	0.2345	0.03406	0.03606	0.1251	0.01413	0.2859
	$A_1/J{\cdot}K^{-2}{\cdot}mol^{-1}$	−0.04865	−0.01181	−0.06441	−0.00281	−0.02307	−0.03406	−0.01778	−0.08571
	$A_2/J{\cdot}K^{-3}{\cdot}mol^{-1}$	0.005542	0.001857	0.006302	−0.00111	0.005118	0.003364	0.006237	0.01220
	$A_3/J{\cdot}K^{-4}{\cdot}mol^{-1}$	−0.00031	$-4.08{\cdot}10^{-5}$	−0.00025	0.000213	−0.0002	−0.00014	−0.00026	−0.00058
	$A_4/J{\cdot}K^{-5}{\cdot}mol^{-1}$	$9.37{\cdot}10^{-6}$	$6.00{\cdot}10^{-7}$	$6.27{\cdot}10^{-6}$	$-1.00{\cdot}10^{-5}$	$5.18{\cdot}10^{-6}$	$3.71{\cdot}10^{-6}$	$5.69{\cdot}10^{-6}$	$1.48{\cdot}10^{-5}$
	$A_5/J{\cdot}K^{-6}{\cdot}mol^{-1}$	$-1.40{\cdot}^{-7}$	$-3.83{\cdot}^{-9}$	$-8.50{\cdot}10^{-8}$	$2.40{\cdot}10^{-7}$	$-6.90{\cdot}10^{-8}$	$-5.20{\cdot}10^{-8}$	$-6.50{\cdot}10^{-8}$	$-1.90{\cdot}^{-7}$
	$A_6/J{\cdot}K^{-7}{\cdot}mol^{-1}$	$7.95{\cdot}10^{-10}$	0	$4.57{\cdot}10^{-10}$	$-2.90{\cdot}10^{-9}$	$3.56{\cdot}10^{-10}$	$2.81{\cdot}10^{-10}$	$2.99{\cdot}10^{-10}$	$9.49{\cdot}10^{-10}$
	$A_7/J{\cdot}K^{-8}{\cdot}mol^{-1}$	0	0	0	$1.40{\cdot}10^{-11}$	0	0	0	0
	%RMS	1.4790	0.3966	0.5027	0.3299	0.1643	0.5971	0.6785	0.4515
	Range/K	12.87–49.53	13.55–50.82	11.77–50.93	12.41–0.52	6.35–54.97	11.87–45.28	7.93–54.75	11.09–53.03
High T Fits	n/mol^{-1}	0.3663	0.1752	0.1852	0.2917	0.2676	0.2535	0.06465	0.18793
	Θ_D/K	977.5376	993.4797	888.4856	629.9682	286.6888	1125.002	223.5839	229.6469
	m/mol^{-1}	0.1172	0.0877	0.1222	0.0991	0.1220	0.1206	0.06579	0.1389
	Θ_E/K	311.4114	260.0957	298.5742	158.368	565.1627	301.8483	352.7505	524.479
	$A_1/J{\cdot}K^{-2}{\cdot}mol^{-1}$	0.005502	0.02315	0.028454	0	0.02266	0.01718	0.04008	0
	$A_2/J{\cdot}K^{-2}{\cdot}mol^{-1}$	$2.20{\cdot}10^{-5}$	0	0	$4.40{\cdot}10^{-5}$	0	0	$-2.90{\cdot}10^{-5}$	$4.04{\cdot}10^{-5}$
	%RMS	0.4415	0.5655	0.347326	0.9901	0.3508	0.5935	0.2623	0.6895
	Range/K	49.53–302.44	50.82–302.62	50.93–302.48	50.52–302.62	54.97–302.42	45.28–302.38	54.75–302.88	53.03–302.89

Table 14
Standard thermodynamic functions of a-SiCH #R337.[a]

T/K	$C_{p,m}/J{\cdot}K^{-1}{\cdot}mol^{-1}$	$\Delta^T S^o_m/J{\cdot}K^{-1}{\cdot}mol^{-1}$	$\Delta^T H^o_m/kJ{\cdot}mol^{-1}$	$\varphi^o_m/J{\cdot}K^{-1}{\cdot}mol^{-1}$[b]
0	0	0	0	0
1	$8.926{\cdot}10^{-5}$	$8.830{\cdot}10^{-5}$	$4.427{\cdot}10^{-8}$	$4.403{\cdot}10^{-5}$
2	$1.884{\cdot}10^{-4}$	$1.797{\cdot}10^{-4}$	$1.818{\cdot}10^{-7}$	$8.881{\cdot}10^{-5}$
3	$3.135{\cdot}10^{-4}$	$2.785{\cdot}10^{-4}$	$4.296{\cdot}10^{-7}$	$1.353{\cdot}10^{-4}$
4	$4.911{\cdot}10^{-4}$	$3.913{\cdot}10^{-4}$	$8.261{\cdot}10^{-7}$	$1.848{\cdot}10^{-4}$
5	$7.600{\cdot}10^{-4}$	$5.277{\cdot}10^{-4}$	$1.442{\cdot}10^{-6}$	$2.393{\cdot}10^{-4}$
6	$1.169{\cdot}10^{-3}$	$6.999{\cdot}10^{-4}$	$2.393{\cdot}10^{-6}$	$3.011{\cdot}10^{-4}$
7	$1.771{\cdot}10^{-3}$	$9.225{\cdot}10^{-4}$	$3.845{\cdot}10^{-6}$	$3.733{\cdot}10^{-4}$
8	$2.614{\cdot}10^{-3}$	$1.211{\cdot}10^{-3}$	$6.016{\cdot}10^{-6}$	$4.592{\cdot}10^{-4}$
9	$3.734{\cdot}10^{-3}$	$1.581{\cdot}10^{-3}$	$9.166{\cdot}10^{-6}$	$5.625{\cdot}10^{-4}$
10	$5.149{\cdot}10^{-3}$	$2.045{\cdot}10^{-3}$	$1.358{\cdot}10^{-5}$	$6.867{\cdot}10^{-4}$
15	0.01849	$6.200{\cdot}10^{-3}$	$6.701{\cdot}10^{-5}$	$1.733{\cdot}10^{-3}$
20	0.04405	0.01474	$2.185{\cdot}10^{-4}$	$3.817{\cdot}10^{-3}$
25	0.08552	0.02864	$5.338{\cdot}10^{-4}$	$7.291{\cdot}10^{-3}$
30	0.15201	0.04968	$1.116{\cdot}10^{-3}$	0.01249
35	0.24679	0.07989	$2.102{\cdot}10^{-3}$	0.01984
40	0.36453	0.12032	$3.622{\cdot}10^{-3}$	0.02977
45	0.49752	0.17080	$5.772{\cdot}10^{-3}$	0.04254
50	0.64998	0.23087	$8.629{\cdot}10^{-3}$	0.05829
60	1.0175	0.38067	0.01690	0.09899
70	1.4466	0.56916	0.02918	0.15225
80	1.9101	0.79231	0.04595	0.21798
90	2.3930	1.0450	0.06745	0.29558
100	2.8877	1.3227	0.09385	0.38422
110	3.3905	1.6214	0.12523	0.48296
120	3.8988	1.9382	0.16167	0.59092
130	4.4102	2.2705	0.20322	0.70724
140	4.9219	2.6160	0.24988	0.83117
150	5.4313	2.9730	0.30165	0.96200
160	5.9360	3.3397	0.35849	1.0991
170	6.4338	3.7145	0.42034	1.2419
180	6.9229	4.0961	0.48714	1.3898
190	7.4021	4.4833	0.55877	1.5424
200	7.8705	4.8750	0.63514	1.6992
210	8.3276	5.2701	0.71614	1.8599
220	8.7732	5.6678	0.80165	2.0239
230	9.2076	6.0674	0.89157	2.1910

Table 14 (*continued*)

T/K	$C_{p,m}$/J·K^{-1}·mol^{-1}	$\Delta^T S^o_m$/J·K^{-1}·mol^{-1}	$\Delta^T H^o_m$/kJ·mol^{-1}	φ^o_m/J·K^{-1}·mol^{-1}[b]
240	9.6308	6.4683	0.98577	2.3609
250	10.044	6.8698	1.0841	2.5332
260	10.446	7.2716	1.1866	2.7077
270	10.839	7.6732	1.2930	2.8842
273.15	10.961	7.7997	1.3274	2.9402
280	11.224	8.0744	1.4034	3.0624
290	11.600	8.4749	1.5175	3.2421
298.15	11.902	8.8006	1.6133	3.3896
300	11.970	8.8744	1.6353	3.4232

[a] All calculated thermodynamic values have an estimated standard uncertainty of less than 0.05 X where X represents the thermodynamic property.
[b] $\varphi^o_m = \Delta^T_\circ S^o_m - \Delta^T_\circ H^o_m/T$.

Table 15
Standard thermodynamic functions of a-SiCH #300.[a]

T/K	$C_{p,m}$/J·K^{-1}·mol^{-1}	$\Delta^T S^o_m$/J·K^{-1}·mol^{-1}	$\Delta^T H^o_m$/kJ·mol^{-1}	φ^o_m/J·K^{-1}·mol^{-1}[b]
0	0	0	0	0
1	$9.011\cdot10^{-5}$	$4.624\cdot10^{-5}$	$2.860\cdot10^{-8}$	$1.763\cdot10^{-5}$
2	$5.737\cdot10^{-4}$	$2.239\cdot10^{-4}$	$3.115\cdot10^{-7}$	$6.815\cdot10^{-5}$
3	$1.837\cdot10^{-3}$	$6.629\cdot10^{-4}$	$1.436\cdot10^{-6}$	$1.842\cdot10^{-4}$
4	$4.253\cdot10^{-3}$	$1.491\cdot10^{-3}$	$4.370\cdot10^{-6}$	$3.979\cdot10^{-4}$
5	$8.166\cdot10^{-3}$	$2.829\cdot10^{-3}$	$1.044\cdot10^{-5}$	$7.408\cdot10^{-4}$
6	0.01389	$4.794\cdot10^{-3}$	$2.130\cdot10^{-5}$	$1.243\cdot10^{-3}$
7	0.02167	$7.491\cdot10^{-3}$	$3.890\cdot10^{-5}$	$1.934\cdot10^{-3}$
8	0.03169	0.01101	$6.539\cdot10^{-5}$	$2.839\cdot10^{-3}$
9	0.04403	0.01544	$1.031\cdot10^{-4}$	$3.985\cdot10^{-3}$
10	0.05864	0.02081	$1.542\cdot10^{-4}$	$5.391\cdot10^{-3}$
15	0.15543	0.06169	$6.744\cdot10^{-4}$	0.01673
20	0.28888	0.12394	$1.772\cdot10^{-3}$	0.03532
25	0.44971	0.20523	$3.609\cdot10^{-3}$	0.06088
30	0.63313	0.30311	$6.307\cdot10^{-3}$	0.09288
35	0.83612	0.41572	$9.973\cdot10^{-3}$	0.13079
40	1.0561	0.54156	0.01470	0.17414
45	1.2894	0.67931	0.02056	0.22251
50	1.5299	0.82759	0.02760	0.27553
60	2.0171	1.1493	0.04532	0.39393
70	2.5118	1.4974	0.06797	0.52644
80	2.9982	1.8647	0.09553	0.67060
90	3.4719	2.2453	0.12789	0.82433
100	3.9339	2.6352	0.16493	0.98586
110	4.3865	3.0314	0.20654	1.1538
120	4.8316	3.4322	0.25264	1.3269
130	5.2704	3.8363	0.30315	1.5044
140	5.7032	4.2428	0.35802	1.6854
150	6.1302	4.6508	0.41720	1.8695
160	6.5508	5.0599	0.48061	2.0561
170	6.9647	5.4695	0.54819	2.2449
180	7.3715	5.8792	0.61988	2.4354
190	7.7707	6.2884	0.69559	2.6274
200	8.1623	6.6970	0.77527	2.8207
210	8.5461	7.1046	0.85881	3.0150
220	8.9220	7.5108	0.94616	3.2101
230	9.2902	7.9156	1.0372	3.4059
240	9.6509	8.3186	1.1319	3.6022
250	10.004	8.7198	1.2302	3.7989
260	10.351	9.1189	1.3320	3.9959
270	10.690	9.5160	1.4372	4.1930
273.15	10.796	9.6406	1.4711	4.2551
280	11.024	9.9108	1.5458	4.3901
290	11.351	10.303	1.6577	4.5873
298.15	11.614	10.622	1.7513	4.7479
300	11.673	10.694	1.7728	4.7843

[a] All calculated thermodynamic values have an estimated standard uncertainty of less than 0.05 X where X represents the thermodynamic property.
[b] $\varphi^o_m = \Delta^T_\circ S^o_m - \Delta^T_\circ H^o_m/T$.

term, its contribution might stabilize the low-k dielectric films and thus increase the decomposition temperature to some extent. However, the enthalpic term is still dominant. We conclude that all the films become thermodynamically metastable at or below their processing temperatures and thus will tend to lose hydrogen during processing.

Table 16
Standard thermodynamic functions of a-SiOCH #844.[a]

T/K	$C_{p,m}$/J·K^{-1}·mol^{-1}	$\Delta_{\circ}^{T}S_m^{\circ}$/J·K^{-1}·mol^{-1}	$\Delta_{\circ}^{T}H_m^{\circ}$/kJ·mol^{-1}	φ_m°/J·K^{-1}·mol^{-1}[b]
0	0	0	0	0
1	$7.242\cdot10^{-5}$	$6.591\cdot10^{-5}$	$3.376\cdot10^{-8}$	$3.215\cdot10^{-5}$
2	$2.102\cdot10^{-4}$	$1.524\cdot10^{-4}$	$1.662\cdot10^{-7}$	$6.930\cdot10^{-5}$
3	$5.124\cdot10^{-4}$	$2.870\cdot10^{-4}$	$5.082\cdot10^{-7}$	$1.176\cdot10^{-4}$
4	$1.139\cdot10^{-3}$	$5.101\cdot10^{-4}$	$1.298\cdot10^{-6}$	$1.855\cdot10^{-4}$
5	$2.326\cdot10^{-3}$	$8.787\cdot10^{-4}$	$2.972\cdot10^{-6}$	$2.843\cdot10^{-4}$
6	$4.381\cdot10^{-3}$	$1.469\cdot10^{-3}$	$6.238\cdot10^{-6}$	$4.288\cdot10^{-4}$
7	$7.666\cdot10^{-3}$	$2.372\cdot10^{-3}$	$1.214\cdot10^{-5}$	$6.376\cdot10^{-4}$
8	0.01256	$3.696\cdot10^{-3}$	$2.211\cdot10^{-5}$	$9.322\cdot10^{-4}$
9	0.01941	$5.550\cdot10^{-3}$	$3.792\cdot10^{-5}$	$1.337\cdot10^{-3}$
10	0.02850	$8.045\cdot10^{-3}$	$6.168\cdot10^{-5}$	$1.877\cdot10^{-3}$
15	0.11400	0.03342	$3.888\cdot10^{-4}$	$7.496\cdot10^{-3}$
20	0.25911	0.08489	$1.301\cdot10^{-3}$	0.01985
25	0.44884	0.16234	$3.054\cdot10^{-3}$	0.04019
30	0.67595	0.26373	$5.852\cdot10^{-3}$	0.06868
35	0.93298	0.38691	$9.863\cdot10^{-3}$	0.10510
40	1.2086	0.52935	0.01521	0.14904
45	1.4892	0.68792	0.02196	0.19997
50	1.7656	0.85917	0.03010	0.25724
60	2.3461	1.2314	0.05060	0.38806
70	2.9684	1.6395	0.07716	0.53729
80	3.6026	2.0773	0.11001	0.70216
90	4.2331	2.5381	0.14919	0.88036
100	4.8528	3.0163	0.19463	1.0699
110	5.4593	3.5073	0.24621	1.2691
120	6.0515	4.0079	0.30377	1.4764
130	6.6292	4.5151	0.36719	1.6906
140	7.1921	5.0271	0.43631	1.9106
150	7.7401	5.5421	0.51098	2.1356
160	8.2733	6.0587	0.59106	2.3646
170	8.7917	6.5759	0.67640	2.5971
180	9.2958	7.0928	0.76685	2.8325
190	9.7858	7.6086	0.86227	3.0703
200	10.262	8.1227	0.96252	3.3101
210	10.726	8.6347	1.0675	3.5515
220	11.178	9.1441	1.1770	3.7941
230	11.618	9.6507	1.2910	4.0377
240	12.047	10.154	1.4093	4.2821
250	12.466	10.655	1.5319	4.5270
260	12.876	11.152	1.6586	4.7723
270	13.278	11.645	1.7894	5.0177
273.15	13.402	11.800	1.8314	5.0950
280	13.671	12.135	1.9241	5.2631
290	14.057	12.622	2.0628	5.5085
298.15	14.366	13.015	2.1786	5.7083
300	14.436	13.104	2.2052	5.7537

[a] All calculated thermodynamic values have an estimated standard uncertainty of less than 0.05 X where X represents the thermodynamic property.
[b] $\varphi_m^{\circ} = \Delta_{\circ}^{T}S_m^{\circ} - \Delta_{\circ}^{T}H_m^{\circ}/T$.

Table 17
Standard thermodynamic functions of a-SiOCH #539.[a]

T/K	$C_{p,m}$/J·K^{-1}·mol^{-1}	$\Delta_{\circ}^{T}S_m^{\circ}$/J·K^{-1}·mol^{-1}	$\Delta_{\circ}^{T}H_m^{\circ}$/kJ·mol^{-1}	φ_m°/J·K^{-1}·mol^{-1}[b]
0	0	0	0	0
1	$2.838\cdot10^{-4}$	$2.821\cdot10^{-4}$	$1.412\cdot10^{-7}$	$1.408\cdot10^{-4}$
2	$5.922\cdot10^{-4}$	$5.707\cdot10^{-4}$	$5.752\cdot10^{-7}$	$2.831\cdot10^{-4}$
3	$9.958\cdot10^{-4}$	$8.820\cdot10^{-4}$	$1.356\cdot10^{-6}$	$4.299\cdot10^{-4}$
4	$1.647\cdot10^{-3}$	$1.249\cdot10^{-3}$	$2.648\cdot10^{-6}$	$5.872\cdot10^{-4}$
5	$2.795\cdot10^{-3}$	$1.728\cdot10^{-3}$	$4.815\cdot10^{-6}$	$7.650\cdot10^{-4}$
6	$4.775\cdot10^{-3}$	$2.397\cdot10^{-3}$	$8.514\cdot10^{-6}$	$9.779\cdot10^{-4}$
7	$7.972\cdot10^{-3}$	$3.355\cdot10^{-3}$	$1.477\cdot10^{-5}$	$1.245\cdot10^{-3}$
8	0.01276	$4.712\cdot10^{-3}$	$2.499\cdot10^{-5}$	$1.589\cdot10^{-3}$
9	0.01942	$6.580\cdot10^{-3}$	$4.091\cdot10^{-5}$	$2.034\cdot10^{-3}$
10	0.02811	$9.058\cdot10^{-3}$	$6.451\cdot10^{-5}$	$2.607\cdot10^{-3}$
15	0.10308	0.03275	$3.691\cdot10^{-4}$	$8.141\cdot10^{-3}$
20	0.22907	0.07861	$1.181\cdot10^{-3}$	0.01955
25	0.39236	0.14668	$2.722\cdot10^{-3}$	0.03781
30	0.58411	0.23477	$5.152\cdot10^{-3}$	0.06304
35	0.80052	0.34076	$8.604\cdot10^{-3}$	0.09494
40	1.0376	0.46294	0.01319	0.13314

Table 17 (*continued*)

T/K	$C_{p,m}$/J·K^{-1}·mol^{-1}	$\Delta_{\circ}^{T}S_{m}^{o}$/J·K^{-1}·mol^{-1}	$\Delta^{T}H_{m}^{o}$/kJ·mol^{-1}	φ_{m}^{o}/J·K^{-1}·mol^{-1}[b]
45	1.2861	0.59944	0.01900	0.17725
50	1.5328	0.74778	0.02605	0.22680
60	2.0640	1.0741	0.04403	0.34030
70	2.5942	1.4321	0.06732	0.47038
80	3.1283	1.8133	0.09593	0.61420
90	3.6661	2.2128	0.12990	0.76948
100	4.2028	2.6268	0.16924	0.93440
110	4.7321	3.0523	0.21393	1.1075
120	5.2483	3.4863	0.26384	1.2876
130	5.7478	3.9262	0.31884	1.4736
140	6.2286	4.3699	0.37874	1.6647
150	6.6901	4.8155	0.44335	1.8599
160	7.1328	5.2615	0.51248	2.0585
170	7.5580	5.7068	0.58594	2.2600
180	7.9672	6.1504	0.66358	2.4639
190	8.3624	6.5918	0.74524	2.6695
200	8.7454	7.0306	0.83079	2.8766
210	9.1181	7.4663	0.92011	3.0848
220	9.4823	7.8989	1.0131	3.2938
230	9.8398	8.3283	1.1097	3.5034
240	10.192	8.7546	1.2099	3.7133
250	10.540	9.1777	1.3136	3.9234
260	10.886	9.5978	1.4207	4.1336
270	11.230	10.015	1.5313	4.3437
273.15	11.339	10.146	1.5668	4.4099
280	11.574	10.430	1.6453	4.5537
290	11.919	10.842	1.7628	4.7634
298.15	12.200	11.176	1.8611	4.9341
300	12.264	11.252	1.8837	4.9729

[a] All calculated thermodynamic values have an estimated standard uncertainty of less than 0.05 X where X represents the thermodynamic property.
[b] $\varphi_{m}^{o} = \Delta_{\circ}^{T}S_{m}^{o} - \Delta_{\circ}^{T}H_{m}^{o}/T$.

Table 18
Standard thermodynamic functions of a-SiOCH #338.[a]

T/K	$C_{p,m}$/J·K^{-1}·mol^{-1}	$\Delta_{\circ}^{T}S_{m}^{o}$/J·K^{-1}·mol^{-1}	$\Delta^{T}H_{m}^{o}$/kJ·mol^{-1}	φ_{m}^{o}/J·K^{-1}·mol^{-1}[b]
0	0	0	0	0
1	$1.865\cdot10^{-4}$	$6.227\cdot10^{-5}$	$4.669\cdot10^{-8}$	$1.558\cdot10^{-5}$
2	$1.521\cdot10^{-3}$	$5.000\cdot10^{-4}$	$7.509\cdot10^{-7}$	$1.245\cdot10^{-4}$
3	$5.504\cdot10^{-3}$	$1.752\cdot10^{-3}$	$3.971\cdot10^{-6}$	$4.286\cdot10^{-4}$
4	0.01366	$4.340\cdot10^{-3}$	$1.316\cdot10^{-5}$	$1.050\cdot10^{-3}$
5	0.02681	$8.705\cdot10^{-3}$	$3.296\cdot10^{-5}$	$2.112\cdot10^{-3}$
6	0.04514	0.01514	$6.852\cdot10^{-5}$	$3.717\cdot10^{-3}$
7	0.06843	0.02378	$1.249\cdot10^{-4}$	$5.939\cdot10^{-3}$
8	0.09622	0.03469	$2.069\cdot10^{-4}$	$8.827\cdot10^{-3}$
9	0.12802	0.04782	$3.187\cdot10^{-4}$	0.01241
10	0.16340	0.06311	$4.641\cdot10^{-4}$	0.01670
15	0.38360	0.16880	$1.805\cdot10^{-3}$	0.04850
20	0.65971	0.31580	$4.392\cdot10^{-3}$	0.09618
25	0.98253	0.49685	$8.479\cdot10^{-3}$	0.15768
30	1.3495	0.70777	0.01429	0.23139
35	1.7566	0.94589	0.02204	0.31615
40	2.1948	1.2088	0.03191	0.41105
45	2.6497	1.4935	0.04402	0.51532
50	3.1059	1.7963	0.05841	0.62814
60	4.0238	2.4430	0.09402	0.87604
70	4.9123	3.1309	0.13875	1.1487
80	5.7306	3.8410	0.19203	1.4407
90	6.4846	4.5601	0.25315	1.7473
100	7.1826	5.2799	0.32153	2.0646
110	7.8322	5.9953	0.39664	2.3894
120	8.4389	6.7031	0.47803	2.7195
130	9.0073	7.4012	0.56529	3.0528
140	9.5414	8.0885	0.65806	3.3880
150	10.045	8.7641	0.75602	3.7240
160	10.520	9.4277	0.85886	4.0598
170	10.970	10.079	0.96633	4.3948
180	11.398	10.718	1.0782	4.7284
190	11.806	11.346	1.1942	5.0602
200	12.197	11.961	1.3143	5.3899
210	12.571	12.565	1.4381	5.7173
220	12.932	13.159	1.5656	6.0421

(*continued on next page*)

Table 18 (*continued*)

T/K	$C_{p,m}$/J·K^{-1}·mol^{-1}	$\Delta_{\circ}^{T}S_{m}^{o}$/J·K^{-1}·mol^{-1}	$\Delta^{T}H_{m}^{o}$/kJ·mol^{-1}	φ_{m}^{o}/J·K^{-1}·mol^{-1}[b]
230	13.280	13.741	1.6967	6.3642
240	13.617	14.313	1.8312	6.6835
250	13.943	14.876	1.9690	7.0000
260	14.261	15.429	2.1100	7.3136
270	14.572	15.973	2.2542	7.6243
273.15	14.668	16.143	2.3003	7.7215
280	14.875	16.509	2.4014	7.9320
290	15.171	17.036	2.5517	8.2369
298.15	15.409	17.460	2.6763	8.4832
300	15.462	17.555	2.7048	8.5388

[a] All calculated thermodynamic values have an estimated standard uncertainty of less than 0.05 X where X represents the thermodynamic property.
[b] $\varphi_{m}^{o} = \Delta_{\circ}^{T}S_{m}^{o} - \Delta_{\circ}^{T}H_{m}^{o}/T$.

Table 19
Standard thermodynamic functions of a-SiOCH #248.[a]

T/K	$C_{p,m}$/J·K^{-1}·mol^{-1}	$\Delta_{\circ}^{T}S_{m}^{o}$/J·K^{-1}·mol^{-1}	$\Delta^{T}H_{m}^{o}$/kJ·mol^{-1}	φ_{m}^{o}/J·K^{-1}·mol^{-1}[b]
0	0	0	0	0
1	$6.773\cdot10^{-5}$	$6.259\cdot10^{-5}$	$3.193\cdot10^{-8}$	$3.066\cdot10^{-5}$
2	$1.851\cdot10^{-4}$	$1.411\cdot10^{-4}$	$1.518\cdot10^{-7}$	$6.523\cdot10^{-5}$
3	$4.186\cdot10^{-4}$	$2.550\cdot10^{-4}$	$4.405\cdot10^{-7}$	$1.082\cdot10^{-4}$
4	$8.650\cdot10^{-4}$	$4.301\cdot10^{-4}$	$1.060\cdot10^{-6}$	$1.652\cdot10^{-4}$
5	$1.656\cdot10^{-3}$	$7.003\cdot10^{-4}$	$2.285\cdot10^{-6}$	$2.433\cdot10^{-4}$
6	$2.956\cdot10^{-3}$	$1.108\cdot10^{-3}$	$4.542\cdot10^{-6}$	$3.512\cdot10^{-4}$
7	$4.947\cdot10^{-3}$	$1.703\cdot10^{-3}$	$8.428\cdot10^{-6}$	$4.993\cdot10^{-4}$
8	$7.806\cdot10^{-3}$	$2.540\cdot10^{-3}$	$1.473\cdot10^{-5}$	$6.993\cdot10^{-4}$
9	0.01169	$3.673\cdot10^{-3}$	$2.438\cdot10^{-5}$	$9.637\cdot10^{-4}$
10	0.01669	$5.153\cdot10^{-3}$	$3.847\cdot10^{-5}$	$1.306\cdot10^{-3}$
15	0.06320	0.01938	$2.216\cdot10^{-4}$	$4.603\cdot10^{-3}$
20	0.14574	0.04809	$7.304\cdot10^{-4}$	0.01156
25	0.25963	0.09227	$1.731\cdot10^{-3}$	0.02303
30	0.40357	0.15189	$3.377\cdot10^{-3}$	0.03933
35	0.57462	0.22663	$5.812\cdot10^{-3}$	0.06057
40	0.76619	0.31569	$9.157\cdot10^{-3}$	0.08675
45	0.96900	0.41757	0.01349	0.11774
50	1.1652	0.52969	0.01882	0.15325
60	1.6093	0.78051	0.03265	0.23640
70	2.0912	1.0645	0.05113	0.33406
80	2.5818	1.3758	0.07450	0.44457
90	3.0665	1.7080	0.10275	0.56633
100	3.5402	2.0557	0.13579	0.69776
110	4.0028	2.4149	0.17351	0.83746
120	4.4558	2.7826	0.21581	0.98418
130	4.9008	3.1569	0.26260	1.1369
140	5.3391	3.5362	0.31381	1.2947
150	5.7712	3.9193	0.36936	1.4569
160	6.1972	4.3054	0.42921	1.6228
170	6.6168	4.6937	0.49329	1.7920
180	7.0296	5.0837	0.56153	1.9641
190	7.4351	5.4746	0.63386	2.1385
200	7.8327	5.8661	0.71020	2.3151
210	8.2221	6.2578	0.79048	2.4936
220	8.6030	6.6491	0.87462	2.6736
230	8.9753	7.0397	0.96251	2.8549
240	9.3387	7.4294	1.0541	3.0374
250	9.6934	7.8179	1.1493	3.2208
260	10.039	8.2048	1.2479	3.4051
270	10.377	8.5901	1.3500	3.5900
273.15	10.482	8.7110	1.3829	3.6484
280	10.706	8.9734	1.4554	3.7754
290	11.028	9.3548	1.5641	3.9613
298.15	11.284	9.6640	1.6550	4.1129
300	11.341	9.7339	1.6760	4.1474

[a] All calculated thermodynamic values have an estimated standard uncertainty of less than 0.05 X where X represents the thermodynamic property.
[b] $\varphi_{m}^{o} = \Delta_{\circ}^{T}S_{m}^{o} - \Delta_{\circ}^{T}H_{m}^{o}/T$.

Table 20
Standard thermodynamic functions of a-SiOCH #149.[a]

T/K	$C_{p,m}$/J·K^{-1}·mol^{-1}	$\Delta_0^T S_m^o$/J·K^{-1}·mol^{-1}	$\Delta^T H_m^o$/kJ·mol^{-1}	φ_m^o/J·K^{-1}·mol^{-1},[b]
0	0	0	0	0
1	$3.482\cdot10^{-4}$	$1.144\cdot10^{-4}$	$8.590\cdot10^{-8}$	$2.848\cdot10^{-5}$
2	$3.387\cdot10^{-3}$	$1.030\cdot10^{-3}$	$1.572\cdot10^{-6}$	$2.444\cdot10^{-4}$
3	0.01244	$3.878\cdot10^{-3}$	$8.896\cdot10^{-6}$	$9.125\cdot10^{-4}$
4	0.02894	$9.535\cdot10^{-3}$	$2.895\cdot10^{-5}$	$2.296\cdot10^{-3}$
5	0.05295	0.01844	$6.929\cdot10^{-5}$	$4.578\cdot10^{-3}$
6	0.08382	0.03072	$1.371\cdot10^{-4}$	$7.865\cdot10^{-3}$
7	0.12048	0.04633	$2.389\cdot10^{-4}$	0.01221
8	0.16166	0.06506	$3.796\cdot10^{-4}$	0.01761
9	0.20692	0.08668	$5.636\cdot10^{-4}$	0.02406
10	0.25552	0.11097	$7.945\cdot10^{-4}$	0.03151
15	0.53143	0.26529	$2.744\cdot10^{-3}$	0.08235
20	0.83285	0.45917	$6.150\cdot10^{-3}$	0.15168
25	1.1401	0.67798	0.01108	0.23473
30	1.4486	0.91309	0.01755	0.32801
35	1.7599	1.1597	0.02557	0.42909
40	2.0753	1.4153	0.03516	0.53631
45	2.3934	1.6781	0.04633	0.64851
50	2.7113	1.9467	0.05909	0.76486
60	3.3397	2.4967	0.08935	1.0075
70	3.9554	3.0580	0.12585	1.2602
80	4.5444	3.6250	0.16837	1.5203
90	5.1027	4.1928	0.21663	1.7857
100	5.6296	4.7579	0.27032	2.0547
110	6.1267	5.3180	0.32912	2.3260
120	6.5964	5.8714	0.39276	2.5984
130	7.0415	6.4172	0.46097	2.8712
140	7.4647	6.9546	0.53352	3.1438
150	7.8684	7.4835	0.61020	3.4155
160	8.2547	8.0037	0.69083	3.6860
170	8.6255	8.5154	0.77524	3.9551
180	8.9822	9.0185	0.86329	4.2225
190	9.3261	9.5135	0.95484	4.4880
200	9.6582	10.000	1.0498	4.7514
210	9.9795	10.479	1.1480	5.0128
220	10.291	10.951	1.2493	5.2720
230	10.592	11.415	1.3538	5.5291
240	10.885	11.872	1.4611	5.7839
250	11.169	12.322	1.5714	6.0364
260	11.445	12.766	1.6845	6.2867
270	11.713	13.203	1.8003	6.5348
273.15	11.796	13.339	1.8373	6.6125
280	11.974	13.633	1.9187	6.7806
290	12.227	14.058	2.0398	7.0243
298.15	12.428	14.400	2.1402	7.2212
300	12.473	14.477	2.1633	7.2657

[a] All calculated thermodynamic values have an estimated standard uncertainty of less than 0.05 X where X represents the thermodynamic property.
[b] $\varphi_m^o = \Delta_0^T S_m^o - \Delta_0^T H_m^o/T$.

Table 21
Standard thermodynamic functions of a-SiOCH #659.[a]

T/K	$C_{p,m}$/J·K^{-1}·mol^{-1}	$\Delta_0^T S_m^o$/J·K^{-1}·mol^{-1}	$\Delta^T H_m^o$/kJ·mol^{-1}	φ_m^o/J·K^{-1}·mol^{-1},[b]
0	0	0	0	0
1	$8.584\cdot10^{-4}$	$8.361\cdot10^{-4}$	$4.200\cdot10^{-7}$	$4.161\cdot10^{-4}$
2	$3.125\cdot10^{-3}$	$1.934\cdot10^{-3}$	$2.125\cdot10^{-6}$	$8.719\cdot10^{-4}$
3	0.01065	$4.407\cdot10^{-3}$	$8.472\cdot10^{-6}$	$1.583\cdot10^{-3}$
4	0.02459	$9.232\cdot10^{-3}$	$2.558\cdot10^{-5}$	$2.837\cdot10^{-3}$
5	0.04412	0.01672	$5.951\cdot10^{-5}$	$4.821\cdot10^{-3}$
6	0.06816	0.02683	$1.153\cdot10^{-4}$	$7.611\cdot10^{-3}$
7	0.09584	0.03937	$1.970\cdot10^{-4}$	0.01122
8	0.12651	0.05414	$3.080\cdot10^{-4}$	0.01564
9	0.15973	0.07094	$4.509\cdot10^{-4}$	0.02084
10	0.19516	0.08958	$6.282\cdot10^{-4}$	0.02676
15	0.39812	0.20574	$2.095\cdot10^{-3}$	0.06609
20	0.62213	0.35083	$4.643\cdot10^{-3}$	0.11867
25	0.84835	0.51391	$8.318\cdot10^{-3}$	0.18117
30	1.0821	0.68905	0.01314	0.25108
35	1.3315	0.87436	0.01917	0.32676

(*continued on next page*)

Table 21 (*continued*)

T/K	$C_{p,m}$/J·K^{-1}·mol^{-1}	$\Delta_0^T S_m^o$/J·K^{-1}·mol^{-1}	$\Delta_0^T H_m^o$/kJ·mol^{-1}	φ_m^o/J·K^{-1}·mol^{-1}[b]
40	1.5954	1.0693	0.02648	0.40730
45	1.8617	1.2726	0.03512	0.49208
50	2.1163	1.4821	0.04508	0.58057
60	2.6686	1.9154	0.06893	0.76660
70	3.1957	2.3670	0.09829	0.96283
80	3.6790	2.8257	0.13270	1.1670
90	4.1326	3.2854	0.17177	1.3768
100	4.5640	3.7434	0.21527	1.5906
110	4.9763	4.1978	0.26299	1.8070
120	5.3707	4.6479	0.31474	2.0250
130	5.7482	5.0928	0.37035	2.2439
140	6.1096	5.5321	0.42965	2.4631
150	6.4561	5.9655	0.49249	2.6822
160	6.7893	6.3929	0.55873	2.9008
170	7.1108	6.8142	0.62824	3.1186
180	7.4224	7.2295	0.70091	3.3355
190	7.7257	7.6389	0.77666	3.5513
200	8.0224	8.0428	0.85540	3.7658
210	8.3139	8.4413	0.93709	3.9789
220	8.6017	8.8347	1.0217	4.1907
230	8.8870	9.2234	1.1091	4.4011
240	9.1709	9.6076	1.1994	4.6101
250	9.4545	9.9877	1.2925	4.8176
260	9.7386	10.364	1.3885	5.0237
270	10.024	10.737	1.4873	5.2284
273.15	10.114	10.854	1.5190	5.2926
280	10.312	11.107	1.5890	5.4317
290	10.602	11.474	1.6935	5.6337
298.15	10.840	11.771	1.7809	5.7974
300	10.895	11.838	1.8010	5.8345

[a] All calculated thermodynamic values have an estimated standard uncertainty of less than 0.05 X where X represents the thermodynamic property.

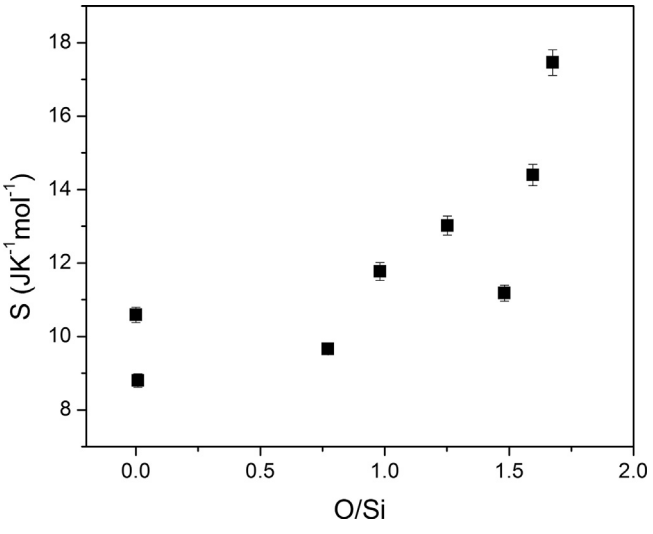

Fig. 4. Standard molar entropy at 298 K for all samples vs. O/Si ratio.

4. Conclusion

Low temperature heat capacity of a-SiOCH and a-SiCH were measured by using a Quantum Design PPMS calorimeter, and hence their standard entropies were obtained. The formation enthalpies, entropies and Gibbs free energies are then obtained with respect to both elements and crystalline constituents/gaseous products. It was found that most of these amorphous materials tend to decompose to their crystalline constituents and gaseous hydrogen at room temperature or processing temperature.

Acknowledgement

Synthesis and partial characterization of the samples were performed at the Logic Technology Development facility of the Intel Corporation in Hillsboro, Oregon, USA. Some characterization and calorimetric measurements at the University of California Davis were supported by Intel Corporation. Salary support for JC came from Intel Corporation and from the A.P. Sloan Foundation's Deep Carbon Observatory. Heat capacity measurements at Brigham Young University were supported by the U.S. Department of

Table 22
Enthalpies of Formation from Compounds ($\Delta H^0_{f,\,comp}$), Entropies of Formation from Compounds ($\Delta S^0_{f,\,comp}$), Gibbs Free Energies of Formation from Compounds ($\Delta G^0_{f,\,comp}$) at Room Temperature and Corresponding Decomposition Temperature for Different Low-k *a*-Si(O)CH Films. A mole is defined as a gram-atom.

Sample #	Film Type	$\Delta_f H^o_{comp}$ (KJ·mol^{-1})	$\Delta_f S^o_{comp}$ (J·K^{-1}·mol^{-1})	$\Delta_f G^o_{comp}$ (KJ·mol^{-1})	T_{decomp} (K)
R337	a-SiCH	−9.57 ± 6.30	−23.85 ± 0.18	−2.45 ± 6.30	401.1
300	a-SiCH	−117.71 ± 2.39	−29.01 ± 0.21	−109.06 ± 2.39	4057.5
844	a-SiOCH	−53.85 ± 1.39	−57.80 ± 0.26	−36.62 ± 1.40	931.7
539	a-SiOCH	10.50 ± 1.41	−58.80 ± 0.22	28.03 ± 1.41	0
338	a-SiOCH	7.44 ± 0.88	−49.78 ± 0.35	22.28 ± 0.88	0
248	a-SiOCH	−33.27 ± 3.01	−44.60 ± 0.02	−19.97 ± 3.01	745.9
149	a-SiOCH	38.19 ± 0.80	−50.29 ± 0.29	53.18 ± 0.80	0
659	a-SiOCH	−83.40 ± 5.24	−41.26 ± 0.24	−71.10 ± 5.24	2021.5

Energy, Office of Science, Basic Energy Sciences, under grant number DE-SC0016446.

Appendix A. Supplementary data

Supplementary data associated with this article can be found, in the online version, at https://doi.org/10.1016/j.jct.2018.08.026.

References

[1] T.A. Pomorski, B.C. Bittel, P.M. Lenahan, E. Mays, C. Ege, J. Bielefeld, D. Michalak, S.W. King, J. Appl. Phys. 115 (2014) 234508.
[2] T.A. Pomorski, B.C. Bittel, C.J. Cochrane, P.M. Lenahan, J. Bielefeld, S.W. King, J. Appl. Phys. 114 (2013) 074501.
[3] N. Suyal, T. Krajewski, M. Mennig, J. Sol-Gel Sci. Technol. 14 (1999) 113–123.
[4] T. Rouxel, G. Massouras, G.-D. Sorarù, J. Sol-Gel Sci. Technol. 14 (1999) 87–94.
[5] T. Rouxel, J.-C. Sanglebœuf, J.-P. Guin, V. Keryvin, G.-D. Soraru, J. Am. Ceram. Soc. 84 (2001) 2220–2224.
[6] G.M. Renlund, S. Prochazka, R.H. Doremus, J. Mater. Res. 6 (1991) 2716–2722.
[7] G.M. Renlund, S. Prochazka, R.H. Doremus, J. Mater. Res. 6 (1991) 2723–2734.
[8] G.D. Sorarù, E. Dallapiccola, G. D'Andrea, J. Am. Ceram. Soc. 79 (1996) 2074–2080.
[9] G.D. Sorarù, S. Modena, E. Guadagnino, P. Colombo, J. Egan, C. Pantano, J. Am. Ceram. Soc. 85 (2002) 1529–1536.
[10] C. Pantano, A. Singh, H. Zhang, J. Sol-Gel Sci. Technol. 14 (1999) 7–25.
[11] S. Martínez-Crespiera, E. Ionescu, H.-J. Kleebe, R. Riedel, J. Eur. Ceram. Soc. 31 (2011) 913–919.
[12] S. Gallis, V. Nikas, M. Huang, E. Eisenbraun, A.E. Kaloyeros, J. Appl. Phys. 102 (2007) 024302.
[13] V. Rouessac, L. Favennec, B. Rémiat, V. Jousseaume, G. Passemard, J. Durand, Microelectron. Eng. 82 (2005) 333–340.
[14] A. Grill, V. Patel, Appl. Phys. Lett. 79 (2001) 803–805.
[15] A.M. Wrobel, P. Uznanski, A. Walkiewicz-Pietrzykowska, B. Glebocki, E. Bryszewska, Chem. Vap. Deposition 21 (2015) 88–93.
[16] S.W. King, D. Jacob, D. Vanleuven, B. Colvin, J. Kelly, M. French, J. Bielefeld, D. Dutta, M. Liu, D. Gidley, ECS J. Solid State Sci. Technol. 1 (2012) N115–N122.
[17] Q. Liu, W. Shi, F. Babonneau, L.V. Interrante, Chem. Mater. 9 (1997) 2434–2441.
[18] G. Trimmel, R. Badheka, F. Babonneau, J. Latournerie, P. Dempsey, D. Bahloul-Houlier, J. Parmentier, G. Soraru, J. Sol-Gel Sci. Technol. 26 (2003) 279–283.
[19] M.A. Schiavon, S.U.A. Redondo, S.R.O. Pina, I.V.P. Yoshida, J. Non-Cryst. Solids 304 (2002) 92–100.
[20] A. Grill, S.M. Gates, T.E. Ryan, S.V. Nguyen, D. Priyadarshini, Appl. Phys. Rev. 1 (2014) 011306.
[21] M.R. Baklanov, J.-F. de Marneffe, D. Shamiryan, A.M. Urbanowicz, H. Shi, T.V. Rakhimova, H. Huang, P.S. Ho, J. Appl. Phys. 113 (2013) 041101.
[22] T. Furusawa, D. Ryuzaki, R. Yoneyama, Y. Homma, K. Hinode, J. Electrochem. Soc. 148 (2001) F175–F179.
[23] M.G. Albrecht, C. Blanchette, J. Electrochem. Soc. 145 (1998) 4019–4025.
[24] F. Iacopi, S.H. Brongersma, B. Vandevelde, M. O'Toole, D. Degryse, Y. Travaly, K. Maex, Microelectron. Eng. 75 (2004) 54–62.
[25] D. Moore, R. Carter, H. Cui, P. Burke, P. McGrath, S.Q. Gu, D. Gidley, H. Peng, J. Vac. Sci. Technol., B 23 (2005) 332–335.
[26] J. Chen, S.W. King, E. Muthuswamy, A. Koryttseva, D. Wu, A. Navrotsky, J. Am. Ceram. Soc. 99 (2016) 2752–2759.
[27] S. Sato, T. Okamura, J. Ye, Surf. Interface Anal. 40 (2008) 1328–1332.
[28] T. Varga, A. Navrotsky, J.L. Moats, R.M. Morcos, F. Poli, K. Müller, A. Saha, R. Raj, J. Am. Ceram. Soc. 90 (2007) 3213–3219.
[29] G. Mera, A. Navrotsky, S. Sen, H.-J. Kleebe, R. Riedel, J. Mater. Chem. A 1 (2013) 3826–3836.
[30] X. Wang, J. Wu, Y. Li, C. Zhou, C. Xu, J. Therm. Anal. Calorim. 115 (2014) 55–62.
[31] A.H. Tavakoli, M.M. Armentrout, M. Narisawa, S. Sen, A. Navrotsky, J. Am. Ceram. Soc. 98 (2015) 242–246.
[32] A.H. Tavakoli, M.M. Armentrout, S. Sen, A. Navrotsky, J. Mater. Res. 30 (2015) 295–303.
[33] F. Danes, E. Saint-Aman, L. Coudurier, J. Mater. Sci. 28 (1993) 489–495.
[34] J. Weiss, H.L. Lukas, J. Lorenz, G. Petzow, H. Krieg, Calphad 5 (1981) 125–140.
[35] M. Nagamori, J.A. Boivin, A. Claveau, J. Mater. Sci. 30 (1995) 5449–5456.
[36] M. Nagamori, I. Malinsky, A. Claveau, MTB 17 (1986) 503–514.
[37] N.S. Jacobson, E.J. Opila, MTA 24 (1993) 1212–1214.
[38] F. Durand, J. Duby, JPE 21 (2000) 130–135.
[39] W.A. Lanford, M. Parenti, B.J. Nordell, M.M. Paquette, A.N. Caruso, M. Mäntymäki, J. Hämäläinen, M. Ritala, K.B. Klepper, V. Miikkulainen, O. Nilsen, W. Tenhaeff, N. Dudney, D. Koh, S.K. Banerjee, E. Mays, J. Bielefeld, S. W. King, Nucl. Instrum. Methods Phys. Res., Sect. B 371 (2016) 211–215.
[40] A. Navrotsky, J. Am. Ceram. Soc. 97 (2014) 3349–3359.
[41] A. Navrotsky, Phys. Chem. Minerals 2 (1977) 89–104.
[42] A. Navrotsky, Phys. Chem. Minerals 24 (1997) 222–241.
[43] R. Stevens, J. Boerio-Goates, J. Chem. Thermodyn. 36 (2004) 857–863.
[44] Q. Shi, J. Boerio-Goates, B.F. Woodfield, J. Chem. Thermodyn. 43 (2011) 1263–1269.
[45] J.M. Schliesser, B.F. Woodfield, Phys. Rev. B 91 (2015) 024109.
[46] E.S.R. Gopal, Specific Heats at Low Temperatures, Plenum Press, New York, 1966.
[47] J.M. Schliesser, B.F. Woodfield, J. Phys.: Condens. Matter 27 (2015) 285402.
[48] B.F. Woodfield, J.L. Shapiro, R. Stevens, J. Boerio-Goates, M.L. Wilson, MRS Proceedings 602 (1999).

JCT 2018-117